Biochimica et Biophysica Acta 1848 (2015) 1868–1885

Contents lists available at ScienceDirect

Biochimica et Biophysica Acta

journal homepage: www.elsevier.com/locate/bbamem

Review

New insights into the molecular mechanisms of biomembrane structural changes and interactions by optical biosensor technology☆

Tzong-Hsien Lee, Daniel J. Hirst, Marie-Isabel Aguilar *

Department of Biochemistry and Molecular Biology, Monash University, Wellington Rd, Clayton, VIC 3800, Australia

ARTICLE INFO

Article history:
Received 19 December 2014
Received in revised form 15 May 2015
Accepted 17 May 2015
Available online 22 May 2015

Keywords:
Dual polarisation interferometry (DPI)
Plasmon waveguide resonance spectroscopy (PWR)
Optical waveguide light mode spectroscopy (OWLS)
Peptide–membrane interaction

ABSTRACT

Biomolecular-membrane interactions play a critical role in the regulation of many important biological processes such as protein trafficking, cellular signalling and ion channel formation. Peptide/protein–membrane interactions can also destabilise and damage the membrane which can lead to cell death. Characterisation of the molecular details of these binding-mediated membrane destabilisation processes is therefore central to understanding cellular events such as antimicrobial action, membrane-mediated amyloid aggregation, and apoptotic protein induced mitochondrial membrane permeabilisation. Optical biosensors have provided a unique approach to characterising membrane interactions allowing quantitation of binding events and new insight into the kinetic mechanism of these interactions. One of the most commonly used optical biosensor technologies is surface plasmon resonance (SPR) and there have been an increasing number of studies reporting the use of this technique for investigating biophysical analysis of membrane-mediated events. More recently, a number of new optical biosensors based on waveguide techniques have been developed, allowing membrane structure changes to be measured simultaneously with mass binding measurements. These techniques include dual polarisation interferometry (DPI), plasmon waveguide resonance spectroscopy (PWR) and optical waveguide light mode spectroscopy (OWLS). These techniques have expanded the application of optical biosensors to allow the analysis of membrane structure changes during peptide and protein binding. This review provides a theoretical and practical overview of the application of biosensor technology with a specific focus on DPI, PWR and OWLS to study biomembrane-mediated events and the mechanism of biomembrane disruption. This article is part of a Special Issue entitled: Lipid–protein interactions.

Contents

1. Introduction . . . 1869
2. Sensor technologies for the real-time measurement of multiple parameters . . . 1870
   2.1. Single versus multi-parameter measurements . . . 1870
   2.2. Plasmon waveguide resonance spectroscopy . . . 1870
   2.3. Optical waveguide light mode spectroscopy . . . 1872
   2.4. Dual polarisation interferometry . . . 1872
3. Membrane preparation and deposition onto the sensor chip surface . . . 1873
4. Characterisation of peptide binding and changes in the bilayer integrity . . . 1874
5. Profiling of lipid perturbation process and disruption by membrane active peptides . . . 1874
   5.1. Antimicrobial peptides . . . 1875
   5.2. Amyloids . . . 1876
   5.3. Apoptotic peptides . . . 1878
6. Kinetic analysis of experimental data to define binding mechanisms . . . 1879
   6.1. Kinetic models . . . 1879
   6.2. Incorporation of birefringence into kinetic models . . . 1880

☆ This article is part of a Special Issue entitled: Lipid–protein interactions.

* Corresponding author.
E-mail address: Mibel.Aguilar@monash.edu (M.-I. Aguilar).

http://dx.doi.org/10.1016/j.bbamem.2015.05.012
0005-2736/

7. Membrane ordering profiles: new insight into biological processes . . . 1881
8. Final considerations and future directions . . . 1882
Transparency document . . . 1883
Acknowledgements . . . 1883
References . . . 1883

1. Introduction

The universal function of the biomembrane is the segregation of different compartments, which enables the cell to establish and maintain essential chemical and electrical gradients between the interior and the exterior environment. Lipid membranes act as an impermeable barrier, limiting the direct crossing of ionic molecules. The maintenance of cell function thus depends on well-controlled material exchange and interplay between peptides/proteins and lipid species in membrane compartments of different functions, leading to the evolution of a wide range of membrane associated channels, transporters, receptors, signalling molecules and cytoskeletons. As a result, energy coupling, cell–cell recognition and communication, immune response, biocompatibility and many other processes are inextricably associated with biomembrane structural integrity.

Biomembranes are complex colloid systems consisting of a wide range of chemical compositions which determine the physical properties of various structures and organisation and therefore underpin the characteristic biological function. The relative amounts of organic components in membranes vary considerably between different organelles and cell types, which contain on a dry weight basis 20–60% protein, 30–80% lipids and up to 10% carbohydrate. The main categories of lipids found in biomembranes are phospholipids, sphingolipids and sterols where phospholipids constitute the major lipid components. These lipid species are subjected to dynamic variation and their relative compositions are tightly controlled and maintained by regulatory networks of lipid composition sensors [1–4]. The physical properties of a lipid membrane such as surface charge, thickness, curvature, elasticity and packing order are highly regulated to maintain the proper function of different membranes [5]. The surface charge of membranes is determined by the relative proportions of phospholipid head groups which are zwitterionic in phosphatidylcholine (PC) and phosphatidylethanolamine (PE) and anionic in phosphatidylserine (PS), phosphatidylinositol (PI), and phosphatidylglycerol (PG). In addition to their effects on surface charges, the different volumes occupied by these head groups and charge–charge repulsion impacts on the membrane curvature and packing density. The bilayer thickness, elasticity and structural packing of lipid molecules in the membrane are mainly affected by the length and degree of unsaturation of the acyl chain. There are also some low abundant phospholipids such as phosphatidylinositides which mediate specific molecular recognition in receptor function, cellular secretion and membrane dynamics [6]. In addition to the phospholipids, the presence of sphingolipids, mainly sphingomyelin and glycosphingolipids, increases the packing density in the membrane resulting in solid–gel phase properties at physiological temperatures [7,8]. Conversely, the sterols interfere with the tight packing of fully saturated acyl chains rendering the membrane in a liquid–crystal state [7]. Due to their condensing effect, sterols reduce the fluidity of membranes composed mainly of phospholipids with unsaturated acyl chains. Thus, modification of the composition of membrane lipids will affect the physiological function of a membrane due to changes in impermeability.

Analysis of biomolecular interactions in the membrane environment is central to understanding biochemical mechanisms. However, the understanding of the complex physicochemical properties of biomembranes continues to be a major challenge in the structural and functional characterisation of peptides/proteins–membrane interactions. Although many analytical systems have been established for measuring inter-molecular interactions such as protein–ligand and protein–protein interactions, these techniques are not readily applicable to characterise the interactions between peptides/proteins and membranes. With recent developments in surface scanning and spectroscopic technologies, the structure, location and orientation of molecules relative to the lipid bilayer, together with the binding affinity and kinetics have been the main focus in exploring the interaction of biomolecules with lipid membranes. These different aspects can be studied by various spectroscopic and surface scanning techniques such as circular dichroism (CD) [9–11], nuclear magnetic resonance (NMR) [12–14], Fourier-transform infra-red (FTIR) [15,16], neutron reflectometry (NR) [17,18], atomic force microscopy (AFM) [19,20], quartz-crystal microbalance (QCM) [21,22], electron microscopy (EM) [23], fluorescence spectroscopy, sum frequency generation spectroscopy [24,25], isothermal calorimetry (ITC) [26,27], surface plasmon resonance (SPR) [28–30], ellipsometry [31–33] and optical waveguide biosensors [34–37].

In spite of this battery of biophysical techniques, there is an enormous gap in our understanding of the membrane-mediated interactions particularly in view of the role of lipid molecular organisation. This is partly due to the lack of knowledge of the structure and physicochemical properties of biomembranes, particularly in terms of the changes in these properties during biomolecule binding, information which is central to characterising the activity of membrane-associated peptides and proteins. Optical biosensors provide label-free real-time qualitative and quantitative measurement of biomolecule–membrane interactions [38]. However, no structural information is provided by commonly used biosensor instruments such as SPR, which is restricted to the measurement of mass-only differences [39]. Thus, whilst it is well-established that the membrane is a fluid environment with a constantly changing structure and composition, the structure of the biomembrane is often the silent, invisible partner in the experimental analysis of membrane-mediated events. However, the optical waveguide techniques [40–42] including dual polarisation interferometry (DPI), plasmon waveguide resonance spectroscopy (PWR) and optical waveguide light mode spectroscopy (OWLS) now provide the advantage of multi-parameter measurements in a single binding assay which yield the optogeometrical properties of density and thickness of the adsorbed layer. The significance of these features lies in the ability to now analyse the impact of membrane active peptides and proteins on the structure of the bilayers simultaneously with the mass changes associated with the binding event.

The aim of this review is to provide a theoretical and practical overview of the application of biosensor technology with a specific focus on DPI, PWR and OWLS to study biomembrane-mediated events. These techniques, which are based on an integrated planar optical waveguide interferometer that combine evanescent field sensing and optical phase difference measurement methods will be described in terms of the specific experimental outputs and the changes in physicochemical parameters of the bilayer that contribute to the sequence of events that leads to the activity of peptides and proteins. Techniques for the preparation and deposition of bilayers onto the sensor chip surface and the quantitative analysis of changes in binding and structural data will be described. The power of these techniques will be illustrated by their application to study a range of biological processes. Finally, new insights into the mechanism of peptide and protein interactions with membranes will be reviewed in terms of the different binding profiles that have been revealed by these techniques. Overall, these techniques allow a new understanding of how membrane characteristics influence peptide and protein function as we can now define membrane interactions in terms of changes in both the structure/orientation of peptides and structure/organisation of membrane lipids which will also impact on the development of new assay technology and drug design.

2. Sensor technologies for the real-time measurement of multiple parameters

2.1. Single versus multi-parameter measurements

Optical techniques have played an important role in the study of the mechanisms and kinetics of molecular interactions in biological processes, with instruments utilising evanescent field sensing to monitor molecular events occurring within 100–200 nm of a surface. Several biophysical techniques have provided important information on the relationship between membrane–active peptide and protein structure and their biological function. SPR was one of the first optical biosensors to be used in the analysis of membrane interactions and several studies yielded detailed analysis of the kinetics and affinity of peptide–membrane interactions. Thus, the concentration measurements and kinetics (association and dissociation) of molecular interaction events have been widely used in delineating the binding mechanisms [28–30]. SPR spectroscopy was also flexible in terms of the membranes studied, being applicable to biomembrane-based systems using planar monolayers, planar bilayers or liposomes [28–30].

Most techniques, including SPR, provide a single parameter measurement in one independent assay based on the widely-used evanescent wave method. As a consequence, the data obtained with these techniques are limited to the measurement of mass-related changes from the resonance angle shift as a function of time. However, the interactions of biomolecules with a membrane involve both the mass-related changes from the binding of peptides/proteins onto the membrane and the impact of this binding on membrane structure. The mass-response from a single measurement can be enhanced or suppressed by the structural changes, for example, due to lateral expansion or compression of the membrane. These structural changes in an anisotropic system (such as a lipid bilayer) can be very complex and difficult to measure without specific labelling. To resolve the binding-promoted membrane structural changes using an optical biosensor, two independent orthogonal polarised fields at a fixed wavelength or two evanescent fields at different optical wavelengths allows the experimental determination of two optogeometrical parameters (average refractive index (RI) and thickness) of a uniform, isotropic thin film. Different configurations of waveguide-based optical sensors have employed either of these two design principles to obtain the layer structure for further studying the dynamic conformational changes associated with membrane binding. These methods include plasmon waveguide resonance spectroscopy (PWR) [43,44], optical waveguide lightmode spectroscopy (OWLS) [37] and dual polarisation interferometry (DPI) [45,46]. The physical basis of these three techniques is depicted schematically in Fig. 1 and are described below.

Spectroscopic ellipsometry is a widely used quantitative method to measure the optogeometrical properties of thin films [47]. The thickness and refractive index (RI) of the adsorbed molecular layer can be derived from the changes in amplitude (Ψ) and phase shift (Δ) of elliptically polarised light upon reflection at solid–liquid interfaces. The adsorbed mass derived from the RI can also be monitored in real-time for kinetic measurements of biomolecular interactions [31–33]. The data analysis requires careful selection of a specific multilayer structural model to calculate the corresponding mass data, followed by data correction via an error minimization process. However, the amplitude Ψ and phase shift Δ can be affected by sample anisotropy and quantitative analysis of this anisotropy has not yet been demonstrated for spectroscopic ellipsometry and requires advanced generalised ellipsometry and more complex fitting models. Thus, whilst ellipsometry yields multi-parameter outputs (i.e., mass, RI, thickness), the assumptions are based on an isotropic layer and methods to analyse anisoptropic properties (e.g. peptide–membrane systems) have not yet been developed. As a consequence, analysis of peptide–membrane interactions by ellipsometry yield accurate mass-only data and cannot be extended to the study of peptide-induced changes in membrane structure which is possible with PWR, OWLS and DPI.

2.2. Plasmon waveguide resonance spectroscopy

Plasmon waveguide resonance (PWR) spectroscopy is a variant of Kretschman-type SPR arrangement that involves more complex assemblies in which surface plasmon resonances in a thin metal (silver) film are coupled with guided waves in a dielectric silicon dioxide overcoating, resulting in excitation of both plasmon and waveguide resonances (Fig. 1a) [42,48]. The optical properties of thin-film materials, such as lipid–protein systems, including the thickness (t) and the complex dielectric constant i.e. refractive index (n) and extinction coefficient (k) can be obtained from the surface resonances upon excitation by both *p*- and *s*-polarised light components. The t, n and k values can be uniquely evaluated from the spectra using a non-linear least-square analysis to fit a theoretical response curve to an experimental curve. These parameters have allowed direct monitoring of the formation and evaluation of the quality of lipid bilayers including lipid rafts [49–51]. When applied to membrane-bound receptors, such as G protein-coupled receptors (GPCRs), PWR provides insight into the dynamic receptor conformational changes associated with the changes in membrane thickness and molecular packing of the lipid molecules resulting from the interactions of structurally different ligands with the same GPCR [42,44]. By measuring the shifts in the spectral resonance minimum for *s*- and *p*-polarisations, different conformational states in the human δ-opioid receptor, cannabinoid receptor and β_2-adrenergic receptor were induced upon binding of structurally different

Fig. 1. Schematic diagrams of optical configuration and data outputs of (a) PWR, (b) OWLS and (c) DPI. (a) The plasmon waveguide resonance spectrometer (PWR) consists of a prism with a silver film overlayered with a SiO_2 film mounted on a rotating table. The method involves the resonant excitation of plasmons by *s* and *p* polarised light from a CW laser. Resonance occurs by varying the angle ϕ at a fixed wavelength and the PWR spectrum is recorded as the reflected light intensity of the electric field of the excitation as a function of the incident angle for both *s* and *p*-polarizations. Molecular layers formed at the interface between the SiO_2 surface and the aqueous compartment interact with this field, thereby altering the resonance excitation process. This results in changes in the intensity of the light reflected by the silver layer measured as a shift of the reflectance angle. A lipid bilayer can be anchored across the hole in the Teflon spacer onto the silica surface and integral membrane proteins can be inserted into the lipid bilayer via detergent dilution. The structural properties (refractive index, thickness, mass per unit area and anisotropy) of the adsorbed lipid bilayer can be characterised and provides a platform for studying the affinity and kinetics of peptide–membrane interactions and ligand–receptor binding. (b) The optical waveguide light mode spectrometer (OWLS) consists of a grated waveguide and a flow cell mounted onto the head of a precision goniometer. The grated waveguide chips are placed on the sensor holder and tightened onto a sealing O ring which forms a flow cell above the waveguide chip. A polarised monochromatic light from a He-Ne laser at a given resonance angle is diffracted by an optical grating at the surface and propagates via total internal reflection inside the waveguide film, generating an evanescent field extending 100–200 nm from the surface. Incoupling of the incident laser beam occurs at two well-defined angles of incidence: one for the transverse electric (TE) and one for the transverse magnetic (TM) mode. Upon rotating the cuvette $\pm 7°$, four characteristic photocurrent peaks (one TE and one TM peak on both the positive and negative sides) can be detected at the incoupling angles αTE and αTM. Changes in the refractive index for the formation of an adlayer of adsorbed biomolecules above the grating waveguide can be monitored in real-time by continuously measuring the shift of these incoupling angles. The changes of thickness and birefringence of the lipid bilayer provide information on the peptide induced membrane structural changes. (c) The dual polarisation interferometer (DPI) consists of a dual slab waveguide guiding light through two high-refractive index structures (sensing waveguide and reference waveguide). Two orthogonal polarisations, TM and TE, pass through the waveguide forming two evanescent fields which are affected by the molecules binding onto the surface. The changes for each TM and TE are detected separately as a phase shift in the fringe pattern at the far-field. Thus, the formation of a unilamellar planar bilayer via liposome adsorption and the dynamic impact of peptide binding on the lipid bilayer structure can be quantitatively analysed in real time. Birefringence is a measure of the difference between the RI parallel to the surface (n_e) and the RI perpendicular to the surface (n_o). The optical birefringence (Δn_f) of a fully aligned/ordered bilayer is larger than that of a disordered unilamellar supported lipid bilayer. Thus, the changes in the packing, alignment and degree of order of lipid molecules assembled on the surface can be determined from quantitative analysis of changes in birefringence. The correlation of membrane-bound peptide mass with bilayer disordering provides new information in delineating the mechanisms of the impact of bound peptides on membrane structure.

ligands including peptide, non-peptide agonists, antagonists and inverse agonists [44,52–56]. PWR has also allowed the determination of the kinetics and thermodynamics of ligand binding to GPCRs for each *p*- and *s*-polarisation and G-protein–GPCR interactions associated with GDP/GTP exchange [43]. PWR can therefore provide unique information on the correlation of ligand structures with distinct ligand-induced changes in the shape and orientation of receptors in the membrane underpinning the functional selectivity in G protein activation.

To characterise the complex spectra obtained with PWR, either spectral simulation or graphical analysis is used to deconvolute the mass and structural changes induced by the molecular interactions in the lipid bilayers [49,57]. Spectral simulation has been used to obtain the structural parameters such as thickness, average surface area per lipid molecule and the degree of long range molecular order of lipid bilayers consisting of single and binary lipids. PWR spectra obtained for the binary mixture of PC (POPC or DOPC) with sphingomyelin (SM) revealed spontaneous lateral segregation of lipids into microdomains with different optical properties generating separate resonance in a PWR experiment with a higher resonance angle for the thicker SM domain and smaller resonance angles for the thinner PC domain [49,57]. The PWR spectra obtained for the incorporation of the GPI-linked protein PLAP into the binary PC/SM lipid bilayers then showed the selective interaction of proteins with the thicker and more tightly packed SM-rich raft microdomain. These analyses further demonstrate the ability of PWR spectroscopy to follow the dynamic sorting of proteins in the membrane bilayer [49,57].

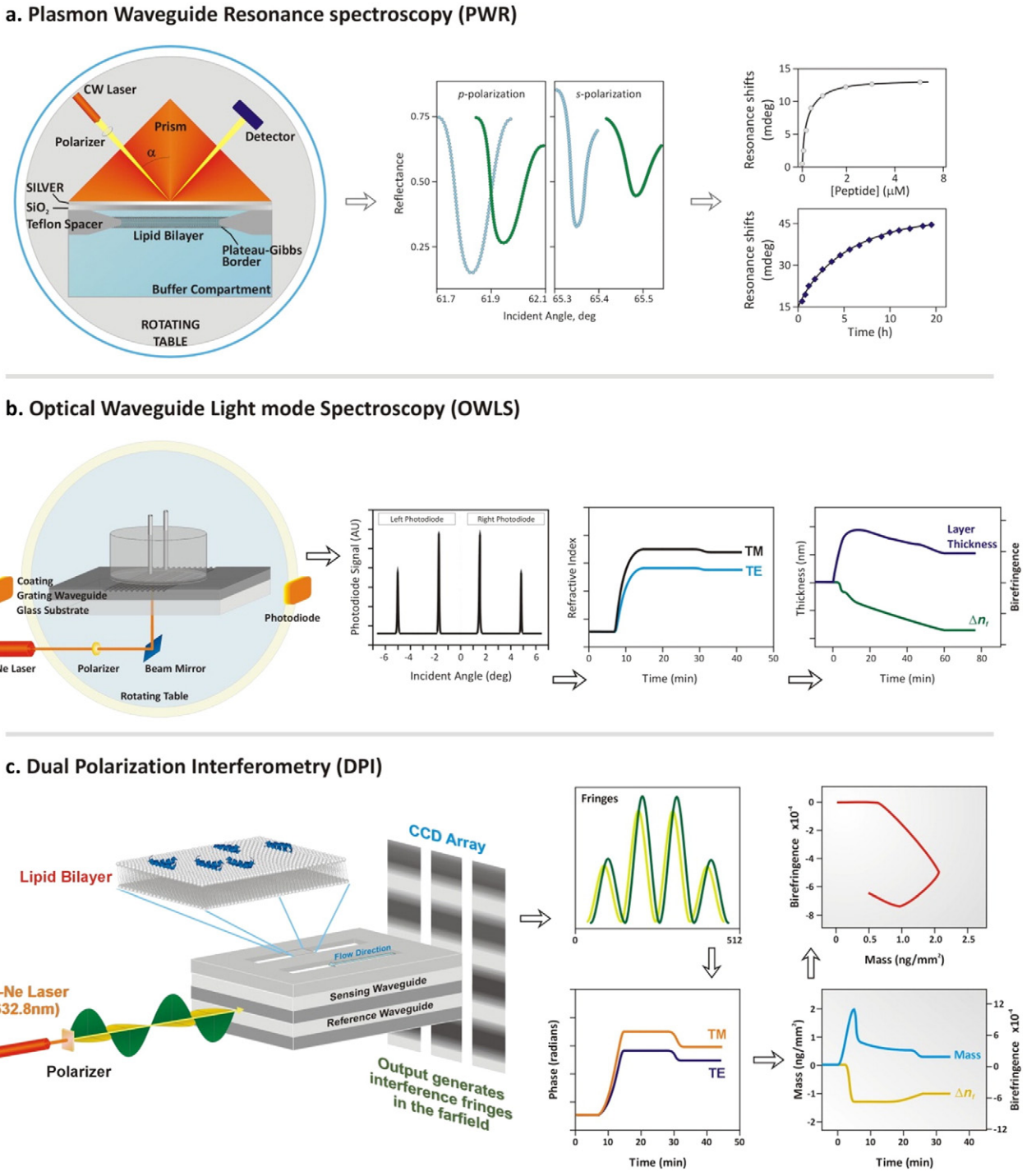

However, this fitting analysis and spectral simulation do not provide a unique determination of the optical parameters for complex spectra obtained from mixed modes of molecular interactions involving multiple conformations that proceed either sequentially or in a parallel series of events. In comparison, the graphical analysis method transforms the plasmon-waveguide resonance spectral shift obtained with both *s*- and *p*-polarised excitation in a (*s*–*p*) coordinate system into a mass-structure anisotropy coordinate system [58–60]. This method provides a simpler and faster route to distinguish between mass and anisotropy changes occurring in the protein–lipid bilayer films than the spectral fitting procedures. The graphical method is thus used to deconvolute a complex sequence of multiple events associated with the mass and structure changes in the system, which cannot be accomplished using the spectral fitting procedure.

This analysis has been demonstrated for the peptide-induced disruption of lipid bilayers from the spectral shift induced by cell-penetrating peptides (CPP), such as penetratin and RL16, binding to eggPC and eggPC/DOPE. Biphasic spectra were obtained for the binding of penetratin to both eggPC and eggPC/DOPE involving two-state binding processes with the mass changes dominant in the first event whilst the second events were attributed to mass (80–90%) and structural (20–10%) changes [58,61]. In contrast, these biphasic changes were not obtained for the binding of penetratin to eggPC/DOPG or the binding of RL16 to eggPC or eggPC/DOPG [58,62]. The membrane interaction and perturbation mechanism of another CPP, RW16, with a range of model membranes including eggPC, DOPC, eggPC/POPG and DOPC/DOPS were also investigated using PWR. Whilst membrane perturbation was observed in each lipid, the affinity constants of RW16 for each bilayer were not affected by the lipid composition [59]. Overall, the structural parameters derived using PWR spectroscopy that include changes in bilayer thickness, anisotropy and average refractive index have provided new insight into the processes by which cell-penetrating peptides modify the membrane structure during their passage through the lipid bilayer.

2.3. Optical waveguide light mode spectroscopy

In optical waveguide light mode spectroscopy (OWLS), a grating is coupled to a planar optical waveguide in which the polarised light is diffracted from the grating and propagated via the internal reflections inside the dielectric slab waveguide (Fig. 1b) [37]. The waveguide is designed to simultaneously excite the zeroth-order transverse electric (TE) and transverse magnetic (TM) polarisation modes when the polarised light excites the waveguide at a particular incident angle. The TE and TM resonance angles are separated from each other and the effective refractive indices of the TM and TE modes can be calculated from those angles. As the evanescent optical waves of the mode extend into the waveguide cover, the adsorption of molecules on the surface results in a shift of the incidence angle for each TM and TE polarisation mode which can be quantitatively monitored in real-time for kinetic analysis. The optogeometrical properties, thickness and refractive index (RI), of the deposited layers can then be extracted from the measured effective refractive index by solving the 3-layer mode equations for the waveguide system. The mass per unit area (mass density) of the adsorbed molecular layer can be calculated from the thickness and RI. The grating-coupled optical waveguides made of silicon titanium oxide ($Si_xTi_{(1=x)}O_2$) are fabricated with sol–gel technology. SiO_2, TiO_2, Ta_2O_5, ITO, ZrO_2 and Al_2O_3, which are applicable to various chemical and biochemical functionalizations, have also been used in the coating on the sensor surface.

The optogeometrical parameters are calculated assuming that the adsorbed layer is uniform (homogeneous) and isotropic. However, lipid bilayers are an optically anisotropic system with a uniaxial optical axis having two different principal refractive indices, the extraordinary (n_e) and ordinary (n_o). The measurement of the difference of n_e and n_o, known as optical birefringence, using the optical waveguide allows the intrinsic structure of the adsorbed biological films to be studied at the sub-nanometre scale since the optical birefringence of a membrane reflects its level of structural organisation [31,63]. OWLS has been used to characterise the adsorption of lipid vesicles onto smooth metal oxide surfaces and the optical anisotropy of phospholipid bilayers with different alkyl chains. It also allows measurement of the temperature dependence of the optogeometrical parameters, thickness, RI and anisotropy of a lipid bilayer [63]. The main phase transition temperature for a planar DMPC bilayer determined by OWLS is around 24 °C which agrees with the value obtained by calorimetry [64,65]. The ability of OWLS to measure the structural properties of lipid bilayers provides a useful way to investigate the membrane partitioning of drugs [66], the dose response of peptide hormones [67], the binding kinetics of peptides and proteins to the bilayer [68,69] and ligand–receptor interactions by incorporating transmembrane receptors [70].

2.4. Dual polarisation interferometry

In DPI, integrated planar optical waveguide interferometers comprise devices with two optical paths that measure optical phase differences combined with evanescent field sensing (Fig. 1c). The light entering the waveguide structure of the interferometer passes through both sensing and reference paths. Two different configurations, Young and Mach–Zehnder interferometry, utilise the wave nature of light to detect changes in the optical properties of a sample [35]. In a typical integrated optical interferometer, the interference of two light beams configured with a Mach–Zehnder format is recombined by directing them to the same path before reaching a photodetector. The intensity of light is thus proportional to the square of the resulting amplitude of two interfering waves. In Young's interferometer, the light emitted from two slits of sensing and referencing paths are projected onto a detector array forming an interference pattern captured by a high resolution recorder unlike in PWR and OWLS where signal intensity is detected by a photodiode detector. In contrast to the common path waveguide interferometer in which the light propagates on the same waveguide (path), DPI comprises a double optical path Young interferometer configuration in which waveguide modes propagate through two vertically stacked single-mode waveguide layers (one sensing and one reference waveguide layers) separated by a layer of cladding material [45,46]. The reference waveguide is buried in the lower cladding layer whilst the sensing waveguide samples the environment through direct contact with the analytes. Polarised light from a laser at a fixed wavelength passes through both waveguides simultaneously producing an interference pattern in the far-field and detected by a CCD camera. Direct measurement of the phase changes is obtained by continuously monitoring the relative phase position of the fringe pattern by performing a Fourier transformation relating intensity to position. The phase changes are related to the changes in the effective RI of the sensing waveguide, allowing the detection of changes above the upper surface of sensing waveguide by the interaction of the evanescent field of the light with the material above the surface. Unlike SPR which only utilises the TM polarisation, DPI is equipped with a polariser switch which measures both the TM and TE polarisation sequentially. Maxwell's equations of electromagnetism for a system of uniform multiple dielectric layers are used to resolve the RI (or density) and thickness of each layer from the absolute effective index of each TM and TE polarisation. The optical anisotropy of a biological film system can also lead to an overestimation of the thickness values in DPI [71]. In these cases birefringence analysis has been developed to allow measurement of the structural organisation of the adsorbed lipid bilayers during their formation and destabilisation by membrane–active peptides and proteins [71–73].

Overall, these optical sensors offer specific features to fully characterise each single lipid bilayer system in terms of a range of dynamic structural parameters including thickness, mass density per unit area, surface area per lipid and molecular orientational order (birefringence

or anisotropy). The ability to accurately measure the orientational order of lipid molecules is a distinctive feature allowing detection and tracking of changes in the structure of the lipid bilayer leading to greater understanding of the impact of biomolecules binding to a biomembrane. The flow-through system also allows kinetic analysis of the binding and membrane disruption process in real time. Since the birefringence quantifies the degree of alignment and uniaxial packing of the lipid molecules on the planar surface, changes in birefringence as a function of peptide binding to the membrane provide unique insight into the mechanism of binding, and the rate and concentration-dependent changes in lipid packing, domain formation and membrane destabilisation.

As outlined in several previous studies [12,33,71–79], the underlying assumptions of DPI data analysis have been well-documented. These studies have shown that determination of both the RI and thickness of the adsorbed film in real time by DPI is valid for a homogenous isotropic adsorbed film. However, this condition is not fulfilled for biomolecular assemblies with highly anisotropic polarizability such as lipid bilayers. The dominating contribution to the optical response for a supported lipid bilayer (SLB) is from the difference in the molecular polarizability of the linearly polarised optical waveguide modes TM and TE. These differences in the polarizability of the two modes lead to three unknown parameters that need to be determined for the SLBs, ie, thickness, refractive index and birefringence (the difference between the effective refractive indices of the two principal axes, or optical anisotropy). However, only two parameters can be determined from two orthogonal polarizations in DPI. To obtain two parameters for three unknown parameters, one of the three parameters is fixed (assumed to be constant). Thus, either RI or thickness is fixed to calculate the birefringence. In order to examine the effect of the molecules on the structural organisation of lipid bilayers adsorbed on a planar solid support, changes in birefringence, thickness and hence mass of the layer were determined by assuming a fixed RI of 1.47 for the bilayer [12,33,71–78]. The birefringence and mass of the bilayer can also be calculated by assuming a fixed thickness of 4.7 nm as used in other works [71,80,81]. However, both theoretical and experimental validations of this assumption has shown that invalid mass and thickness values are derived if an isotopic adlayer model is used (without taking the anisotropy into account) [71, 77,79]. A number of studies have therefore used the thickness to define the quality of the deposited membrane and then focused on changes in birefringence during peptide binding. This approach has revealed more details about the effect of the peptide on the membrane structure than a change in thickness and allows the mechanism of action to be more clearly defined as outlined in the Sections below.

A subject of intense debate has been the presence and thickness of a stratified water layer between the substrate and supported bilayers. The calculation of the water layer between the substrate and the supported bilayer has been compared using DPI and QCM-D [82]. It was reported that the mass of only the DOPC bilayer excluding the mass of any solvent incorporated in the bilayer could be resolved by DPI. The mass contribution of the coupled solvent between the DOPC bilayer and the solid support was measured by QCM-D. By comparing these two methods, the thickness of the hydration layer was 10.46 ± 0.15 Å for trapped D_2O and 10.21 ± 0.40 Å for trapped H_2O. The DPI measurement is insensitive to solvent, thus only the mass of lipid bilayer adsorbed to the surface is determined and does not include the bulk solvent or the trapped layer of hydration which can impact on the measurements by other methods.

3. Membrane preparation and deposition onto the sensor chip surface

The investigations of membrane-mediated processes have advanced the development of model membrane systems that allow interrogation with various biosensing methods. In order to fully exploit these specific features of waveguide-based optical sensors (DPI, OWLS and PWR) to study peptide–membrane interactions, it is essential to establish membrane preparation protocols which provide structurally defined defect-free membranes with highly reproducible properties. Although the heterogeneous and complex components in natural biomembranes directly isolated from cells of living organisms are the ideal template, use of those membranes in a biosensor environment is technically challenging. As a result, artificial membrane model systems are used, which still provide valuable complementary information on the physicochemical properties and structural roles of individual lipids in membrane-related activity and the effects of lipid bilayers on the binding characteristics, structure and activity of peptides and proteins. Supported lipid bilayers and tethered liposomes are two of the most commonly used membrane models in studying membrane–mediated processes. Supported lipid bilayers, which are physisorbed onto a planar substrate, provide the most applicable and direct method for optical biosensing systems.

Several methods have been commonly used for the formation of supported lipid bilayers (SLBs) on the surfaces of either unmodified or chemically modified sensor chips. In the first type of solid supported membrane, lipid bilayers are adsorbed onto a hydrophilic surface by transferring a lipid monolayer formed at the air–water interface using the Langmuir–Blodgett and Langmuir–Schaefer deposition techniques [83,84]. This method has been used to prepare the lipid bilayers for the OWLS system [63]. The properties of the adsorbed bilayer prepared by the Langmuir–Blodgett (LB) techniques are strongly dependent on the preparation of a stable, well-compressed and homogeneous lipid monolayer on the Langmuir trough. It also provides advantages in preparing asymmetric bilayers with a different lipid composition in each monolayer and incorporating lipids with large chemically-modified head groups such as lipopolysaccharides in the outer monolayer only. The residual organic solvent used in the spreading of lipid solution on water is the one of the main concerns in preparing the bilayers with highly reproducible packing organisation. Incorporation of proteins into the bilayers can be complicated by denaturation as they may be exposed to air before transferring with the monolayer. An alternative way to incorporate proteins is via fusion of receptor-associated vesicles or micelles into the already deposited lipid bilayers.

A second method for preparing the lipid bilayers on a chip surface involves the adsorption and fusion of unilamellar lipid vesicles from an aqueous suspension onto the substrate [83,84]. This is a relatively easy and direct method which has been used to prepare lipid bilayers in OWLS and DPI systems as shown in Fig. 2. Several factors can affect the adsorption, collapse and fusion/spreading of lipid vesicles into bilayers [83–85]. These factors involve the type, smoothness and cleanness of the substrate; types, pH and ionic strength of buffer; adsorption temperature; size, composition, surface charge and concentration of the lipid vesicles. The addition of 1–2 mM Ca^{2+} or Mg^{2+} is also critical to assist the adsorption of lipid vesicles and stabilisation of final lipid bilayers [85]. Understanding the role of these factors allows the establishment of experimental conditions to obtain a defect-free unilamellar bilayer and to avoid the imperfect structural mixture of vesicles and bilayers on the chip surface. The formation and final structural properties of SLBs consisting of a wide range of lipid compositions have been fully characterised by DPI and OWLS [63,71,78].

An alternative way to prepare supported lipid bilayers is via preparation of a black lipid membrane [44,86]. As in PWR, the lipid bilayers are formed in a small Teflon orifice separating two compartments containing aqueous solutions. Lipids dissolved in organic solvent spread across the Teflon orifice, resulting in the initial orientation of lipid head groups towards the silica surface in the prism. An annular plateau-Gibbs border of lipid solution anchoring the membrane to the Teflon spacer is formed after the addition of aqueous buffer into the sample cell. This border of lipids provides membrane flexibility allowing the bilayer to expand and deform upon the insertion of peptides and proteins.

The ability to characterise bilayer formation in real time prepared by different methods by PWR, OWLS and DPI is important to determine the experimental conditions to control the structural properties of the

bilayer. Each single planar bilayer system can therefore be fully characterised in terms of a range of dynamic structural parameters including thickness/density, mass, lipid surface area, and orientational order. The values of selected structural properties for lipid bilayers of various compositions using DPI are listed in Table 1. These values correlate closely with the reported values obtained from X-ray reflectivity and neutron reflectivity studies [87]. This degree of quantitative characterisation of the bilayer structure enables the real time action of membrane-active peptides and proteins to be accurately probed in terms of alterations in the dynamic structure of the bilayer.

In addition to the unilamellar bilayer adsorbed onto the chip surface, membranes have also been tethered onto modified chips as tethered liposomes [76,80]. The tethered liposome not only allows the incorporation of transmembrane receptors to study ligand-induced receptor activation/inhibition, but also allows for the membrane destabilisation mechanisms by insertion or rupture induced by peptides/proteins to be differentiated.

Understanding the role of dynamic transbilayer asymmetry is of particular importance in exploring the relationship between biomembrane structure and various cellular processes and in engineering biomembranes as biomaterials. Studies have demonstrated the asymmetric distribution of lipid composition in SLBs can be formed via direct vesicle adsorption–fusion [88–90]. The extent of lipid mobility, lateral distribution and transbilayer asymmetry of the SLBs is highly dependent on the lipid composition (charge density, acyl chain length and degree of unsaturation and classes i.e. phospholipids, sphingolipids, sterols). Lipid asymmetry is also strongly affected by the physical properties of underlying solid surfaces, membrane preparation methods, vesicle fusion conditions and can vary within typical experimental timescales. For example, the mobility of PS in lipid bilayers formed on TiO_2 is restricted in the presence of calcium ions whilst the mobility of zwitterionic PC is not affected [51]. In contrast, both PC and PS are mobile in the bilayer formed on SiO_2. The preparation of stable asymmetric bilayers therefore remains challenging in terms of producing well-controlled and reproducible SLBs. Bilayer asymmetry can also be induced by the phospholipid molecules binding to the SLBs. For example, the methyl-β-cyclodextrin-mediated lipid exchange technique has been applied to prepare asymmetric SLBs containing sphingomylin and can also be prepared in the presence of a reconstituted glycosylphosphatidylinositol-anchored protein [75]. DPI and QCM-D have also been used in combination to monitor the mass and birefringence changes for lipid flip-flop induced by the temperature-dependent phase transitions in asymmetric SLBs on TiO_2 [91].

4. Characterisation of peptide binding and changes in the bilayer integrity

The changes in the optical thickness and mass obtained in real time represent an overall signal response corresponding to the layer formation. This mass or thickness alone does not reveal the dynamic changes in the structure of the lipid bilayers. Amongst various types of thin films, phospholipid bilayers show differences in RI for two orthogonal polarisations owing to the liquid crystal properties of lipid molecules self-assembled into uni-axial aligned bilayers. The ordered orientation of lipid molecules in a membrane therefore creates an anisotropic system with a unique optical anisotropic property, where two principal RIs, ie, n_e and n_o in a uniaxial optical axis are different. The difference between these two RIs for a lipid film is defined as the birefringence (Δn_f) as $\Delta n_f = n_e - n_o$. Thus, the degree of molecular order, S, of the uniaxial lipid bilayer is defined by the ratio of the principal polarizabilities of the bilayer to the molecular polarizabilities [86]. This order parameter (S) is proportional to the birefringence values. Thus, the birefringence values represent an averaged measurement of lipid molecular orientation order and the lipid acyl chain packing order. High Δn_f values are obtained for a fully aligned lipid bilayer whereas low Δn_f indicates a random and disordered lipid bilayer. The birefringence values obtained for planer lipid bilayers with various compositions are shown in Table 1. A typical bilayer has a birefringence of 0.01–0.02 refractive index units. The values are higher in the bilayers with fully saturated acyl chains than in those bilayers with unsaturated acyl chains. DPI can measure refractive index increments with high sensitivity and can therefore characterise very subtle dynamic changes in orientation and packing order of lipid molecules, revealing mechanisms of interaction that are difficult if not impossible to see by other means. In summary, birefringence provides a direct measurement of the quality of the bilayer itself and changes in the birefringence value reflect changes in the bilayer structure as it undergoes phase transitions or interactions with other molecules such as proteins, polymers or ions. The ability to measure birefringence is the most significant feature of the DPI instrument in terms of investigating membrane-mediated events.

The ability of a waveguide-based biosensor to measure both mass and birefringence simultaneously allows the analysis of the relationship between the two properties to be measured in the interactions between peptides/proteins and lipids. In the first instance, plots of mass versus time (Fig. 1c) yield information on binding which is analogous to other optical biosensors such as SPR. However, dependence of birefringence on time (Fig. 1c) provides new information on the simultaneous changes in membrane structure during the binding event. More significantly, the combination of these plots to give the birefringence vs. mass plots (as illustrated in Fig. 3) reveals an enormous amount of new information. In particular, a number of transitions can be described which can be used to evaluate peptide behaviour and mechanism of action. Both the initial binding of an analyte (such as a peptide), and any subsequent processes, may affect both the mass and structural ordering of the membrane, and the relationship between the two can be visualised using the plot of birefringence vs. mass. Binding always involves some increase in mass (at least initially) and may also be accompanied by changes in birefringence. For a decrease in birefringence (and hence and increase in membrane disorder), changes in the slope of the birefringence–mass graph provides a measure of the effect that bound molecules have on a membrane—from a horizontal to shallow slope representing a surface binding that has only a small effect on birefringence, through a near vertical decrease for a substantial interruption of the membrane structure, with other cases that fall between the two extremes (Fig. 3). Alternatively, binding may also cause an increase in birefringence, suggesting that a stabilising or ordering effect is occurring. Membrane changes subsequent to binding may include dissociation from the membrane with recovery in birefringence or mass loss with further decreases in order. This last possibility may indicate normal dissociation combined with a slow decrease in birefringence from peptide already bound, or it may indicate the loss of mass from the surface, either by membrane thinning and spreading or the removal of material from the surface. With the study of appropriate model systems, it may become possible to characterise peptide–membrane interactions directly by observing the dynamic relationships between mass and structural organisation. This would be an extremely powerful method for enhancing understanding of peptide–membrane interactions.

5. Profiling of lipid perturbation process and disruption by membrane active peptides

Analysis of mass-birefringence plots, derived from the phase changes of DPI and (s, p) coordinate systems, containing both mass and structural axis placed according to the sensitivity factor of the PWR sensor reveals the changes in membrane ordering that occur during peptide binding. Such mass-birefringence analysis allows very detailed and subtle differences in the interactions between different lipid membranes and peptide sequences to be defined. This graphical analysis of the correlation between binding and structural changes has been used to evaluate the accumulated impact of a number of peptides to effect progressive changes in membrane structure. The birefringence analysis provides unique real-time information on the impact of peptides on

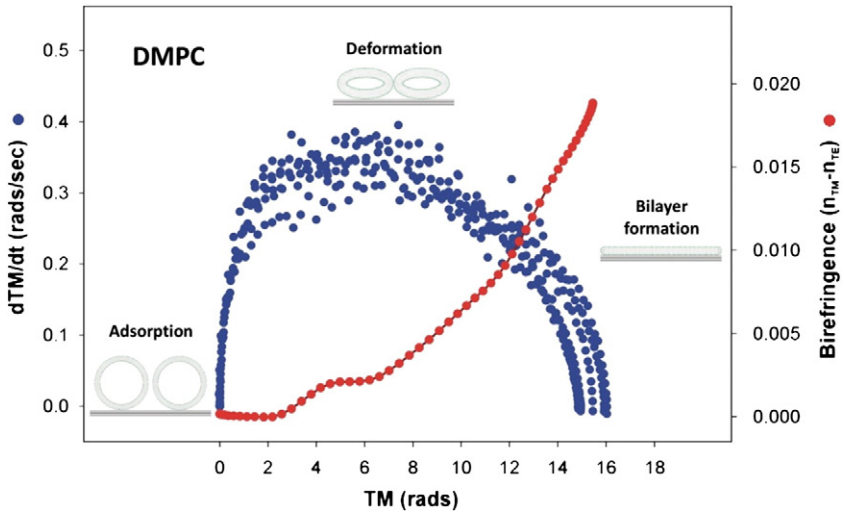

Fig. 2. The kinetics of bilayer formation via direct liposome adsorption characterised by DPI. A faster rate of liposome adsorption is obtained within the first few seconds of injection. The adsorption rate slows down as more liposomes saturate the chip surface where collapse or deformation of liposomes occurs and the birefringence increases. The rate drops to nearly zero as the bilayer forms on the surface with a high birefringence.

the changes in organisation occurring within a lipid bilayer, and assists in describing the behaviour of membrane-active peptides when interacting with membranes of different lipid compositions. Knowledge of the membrane structure changes significantly informs our understanding of biological processes categorised based on their activity in membrane environment with specific examples including antimicrobial peptides, amyloid peptides and apoptotic peptides are described below.

5.1. Antimicrobial peptides

Antimicrobial peptides (AMPs) are a class of peptides which act against pathogenic microorganisms, mostly by a direct-killing mechanism, but some AMPs act as immunomodulators in chemotaxis, angiogenesis and regulation of the T cell response. The membranes of pathogens have been considered as the main target of AMPs for their direct-killing activities. The interaction of AMPs with a membrane can result in structural and topological changes in peptides and perturbation of membrane integrity. Complex factors determine the activities of AMPs in destabilising membrane structure and function and the ability of AMPs to discriminate between pathogen and host cell membranes. Delineating the mechanisms of AMPs action thus requires the dynamic changes in membrane structure to be characterised quantitatively in response to the peptide structural properties. Various molecular models have now been used to describe the AMP action on membrane. As reviewed earlier [94,96], the molecular models range from structurally defined classical mechanisms such as barrel-stave, toroidal and detergent-like carpet models to structurally less defined non-membranolytic mechanisms, such as sinking raft [32,97], lipid

Table 1
Structural properties of unilamellar SLBs determined using DPI.

Lipids	Ratio	Thickness (Å)	Birefringence	Mass (ng/mm^2)	Reference
DMPC	100	45.2 ± 0.7	0.0217 ± 0.0006	4.53 ± 0.08	[73,78]
DMPC/DMPG	80:20	47.6 ± 1.6	0.0235 ± 0.0015	4.77 ± 0.16	[73,78]
DMPC/DMPG/Chol	64:16:20	34.6 ± 0.6	0.0164 ± 0.0003	3.47 ± 0.07	[73]
DMPE/DMPG	80:20	43.7 ± 5.0	0.0244 ± 0.0028	4.34 ± 0.49	[73]
DMPC/DMPS	80:20	47.5	0.0231	4.75	[73]
POPC	100	48.7 ± 1.5	0.0185 ± 0.0007	4.71 ± 0.15	[71,72]
POPC/POPS	80:20	46.9 ± 0.6	0.0195 ± 0.0001		[71]
POPC/POPS	75:25	38.1 ± 6.0		4.07 ± 0.20	[92]
POPC/POPG	80:20	45.4 ± 0.4	0.0177 ± 0.0011	4.56 ± 0.05	[72]
POPC/POPS/POPE	60:30:10	46.9 ± 1.3	0.0176 ± 0.0015	4.70 ± 0.12	
POPC/POPS/POPE	60:20:20	47.9 ± 0.1	0.0197 ± 0.0002	4.79 ± 0.01	
POPC/POPE/POPS/PI	50:30:10:10	44.8 ± 0.6	0.0176 ± 0.0005	4.47 ± 0.07	[93]
POPC/POPE/POPS/PI/CL	48:20:10:10:4	48.9 ± 1.8	0.0198 ± 0.0001	4.88 ± 0.33	[93]
POPE/POPG	80:20	42.5	0.0226	4.25	
DOPC	100	46.0 ± 3.0	0.0170 ± 0.0010	4.60 ± 0.30	[76]
		46.7 ± 2.6	0.0149 ± 0.0005	4.70 ± 0.23	[94]
DOPG	100	34.7 ± 3.9	0.0124 ± 0.0025	3.30 ± 0.54	[94]
DOPC/DOPE/DOPS	20:50:30	52.0 ± 3.0	0.0191 ± 0.0007	5.20 ± 0.30	[76]
DOPC/DOPE/DOPS	50:20:30	46.0 ± 2.0	0.0172 ± 0.0004	4.60 ± 0.20	[76]
DOPC/DOPS	80:20	52.9 ± 0.1	0.0250 ± 0.0019		[71]
	70:30	45.0 ± 4.0	0.0158 ± 0.0002	4.52 ± 0.04	[76]
DOPE/DOPG	75:25	45.0 ± 3.0		4.40 ± 0.30	[32,75]
SoyPC/DOPE/Chol	60:30:10	46.3	0.0135	4.63	[95]
LPS on DOPE/DPOG				0.7	[32]
E. coli extract		58.3 ± 1.3	0.0195 ± 0.0020	5.83 ± 0.07	[73]

segregation into domains [59,76,77], and formation of non-lamellar phases [8,20,41]. When considering these models it is possible that multiple modes of action may be present simultaneously, and that the mode of action (if any) may be dependent on variable factors such as the concentration of peptides in solution and membrane-bound, the lipid membrane composition and structure, the kinetics of binding and structural changes of all interacting partners.

The structural characteristics of an adsorbed lipid bilayer obtained from the DPI waveguide-based biosensor offers a unique quantitative analysis of membrane perturbation mechanisms for AMP action. Most AMP binding results in an essentially linear decrease in the bilayer birefringence with increasing peptide mass bound to membrane. As shown in Fig. 3 for HPA binding to DMPC/DMPG (80:20) and citropin 1.1 binding to DMPC, this decrease in birefringence immediately after peptide binding is a characteristic pattern for peptides incorporated into the membrane without a threshold on the membrane surface [78]. These patterns have been observed for aurein 1.2 binding to *E. coli* lipid extract and DMPE/DMPG [73], HPA3 and HPA3P binding to DMPC and DMPC/DMPG [78], peptides derived from various coagulation factors binding to DOPE/DOPG [33], C-terminal peptides from S1 peptidases to DOPE/DOPG [33], novicidin to DOPC/DOPG [98], KYE28, KYE21 and NLF binding to DOPE/DOPG [75], citropin 1.1, maculatin 1.1 and caerin 1.1 binding to DMPC [99]. However, this linear decrease in birefringence with increased peptide mass seen in one membrane can become more complex with changes in either peptide sequence or changes in lipid composition. The binding of HPA3 and maculatin 1.1 to the gel-DMPC bilayer displayed similar linear behaviour with bilayer structural disordering [12,17,72,78]. However, the helical kink in maculatin 1.1 induces a biphasic change with initial increases in membrane-bound peptide mass without significant bilayer disorder followed by an abrupt non-linear disordering with further increases in mass upon binding to the fluid DMPC bilayer (Fig. 3). In contrast, the linear helical HPA3 showed a linear decrease in bilayer order with the gel-DMPC/DMPG bilayer (Fig. 3). These studies clearly demonstrated that the role of proline in bilayer perturbation can be delineated by the changes in birefringence which is not possible by mass-only measurements. These distinctively different features in binding to DMPC/DMPG, despite similar binding behaviour with DMPC between HPA3 and maculatin 1.1, also demonstrate the importance in differentiating the membrane structural changes from the peptide binding, since in the absence of the birefringence data, the main conclusion would be that both peptides have similar binding mechanisms.

The birefringence–mass profiles can also provide significant new insight that redefines current models of AMP action [73,74,99]. In particular, the sequential steps of binding, insertion and bilayer disruption can be examined in real time at continuous increments of peptide:lipid (P:L) ratio. Whilst many studies focus on defining the critical concentration for membrane destruction, characterising the steps associated with different extents of bilayer perturbation at a distinctive P:L threshold provides a much clearer understanding of the action of AMPs on the membrane. Aurein 1.2 and magainin 2 are naturally found in the dorsal secretion of an Australia tree frog and an African frog, respectively. Despite the difference in sequence and in particular the length, with 13 and 23 amino acids for aurein 1.2 and magainin 2, respectively, both peptides adopt an amphipathic helix in an anionic membrane environment, whilst no structure was found for magainin2 in a neutral membrane environment. The carpet mechanism has been proposed as the mechanism by which both peptides lyse membranes based on similar critical peptide:lipid (P:L) ratios measured by conventional means. However, DPI can provide information on membrane structure changes immediately prior to, during and after membrane lysis and significant differences are apparent for these two peptides which are described as acting by the same mechanism. Firstly, the P:L ratio determined at the point of disruption for an anionic membrane was markedly lower for aurein 1.2 than for magainin 2 (Fig. 3 & Table 2). Moreover, an alanine-substituted analogue, $Ala^{8,13,18}$-mag2 with enhanced bactericidal activity also showed anionic membrane disruption at a P:L ratio similar to magainin 2. However, the $Ala^{8,13,18}$-mag2 also disrupted the neutral DMPC membrane (Figs. 3 & 4) at nearly double the P:L ratio. From the P:L ratio determined at the point of membrane disruption, a "carpet mechanism" would be simply attributed to the mechanisms of action of these frog peptides. However, the drop in birefringence was reversible for aurein 1.2 after its disruption of both neutral DMPC and anionic DMPC/DMPG membranes [73,74,99]. In contrast, a partially reversible birefringence drop with permanent disordering was obtained for $Ala^{8,13,18}$-mag2 after membrane disruption. These partially reversible birefringence changes with membrane disruption correlated with the peptide insertion and bilayer expansion as evident from AFM studies (Fig. 4) and both fluorescence dye release and AFM results showed that aurein 1.1, magainin 2 and $Ala^{8,13,18}$-mag2 disrupt the membrane differently [73,74,99]. Overall, these experiments clearly demonstrate that definition of AMP action in terms of a specific model is too simplistic. In particular, the reversible packing disorder–order behaviour observed for different bilayers is quite distinctive for various AMPs, behaviour which is not apparent with other spectroscopic techniques. The analysis of membrane disordering has therefore extended our understanding of how the membrane undergoes a reversible structural change upon exposure to antimicrobial peptides and how the bilayer can either recover or, at a critical peptide concentration, begins to disintegrate.

The activity of antibacterial polymers on the SLBs has been monitored by the in situ changes of optical birefringence obtained by OWLS [77]. The calculation of layer thickness and birefringence values was based on an anisotropic adlayer model whilst the correlation of layer thickness and birefringence was assessed comparatively with a composite/exchange model. The addition of antibacterial polymer to a bilayer resulted in initial increases in thickness from 5.2 nm to 8 nm and decreased to 5.8 nm whilst the birefringence decreased from 0.026 to −0.06. This clearly showed the disordering effect and lipid disintegration in response to the antibacterial polymer. Based on the composite model, the surface coverage of antibacterial polymer in the final structure was also calculated with less than 40% of the area covered with lipids at the end of the measurement.

Selectivity towards specific target cells is crucial to develop new AMPs and other therapeutic agents acting on the membrane. The binding of peptides to model membranes with known lipid composition and structural properties has demonstrated the complex interplay between charge, hydrophobicity, amphipathicity, bilayer structural organisation, presence of sterol, sphingomyelin and sterol etc. in mediating binding selectivity. In addition, modification of peptide sequence, length, end-tagging with a stretch of either charged or hydrophobic residues can also enhance the selection towards pathogenic bacteria without toxicity towards host cells. Studying the selective binding of peptides to naturally occurring cell membrane is still limited to whole cell binding assays and liposomes derived from cell membranes. The preparation of natural membranes on solid supports for biosensor applications still remains a challenge in terms of their stability and reproducibility.

What we can conclude is that these peptides have significantly different binding properties and that these differences relate to differences in the effect on membrane structure, and that the bioactivity of these peptides is likely to be mediated by significant changes in membrane structure, which has not been previously demonstrated. More direct correlations will be possible when birefringence measurements of bacterial membrane extracts are performed.

5.2. Amyloids

The association of misfolded protein and peptide aggregates with neuronal cell membranes may play a key role in their neurotoxicity in several degenerative disorders, but the underlying mechanisms of amyloid growth and toxicity are still not fully understood. Formation of amyloid aggregates has been studied by DPI which showed that aggregation is mediated by various types of surfaces and the kinetics of aggregation is significantly enhanced upon adsorbing on a hydrophobic

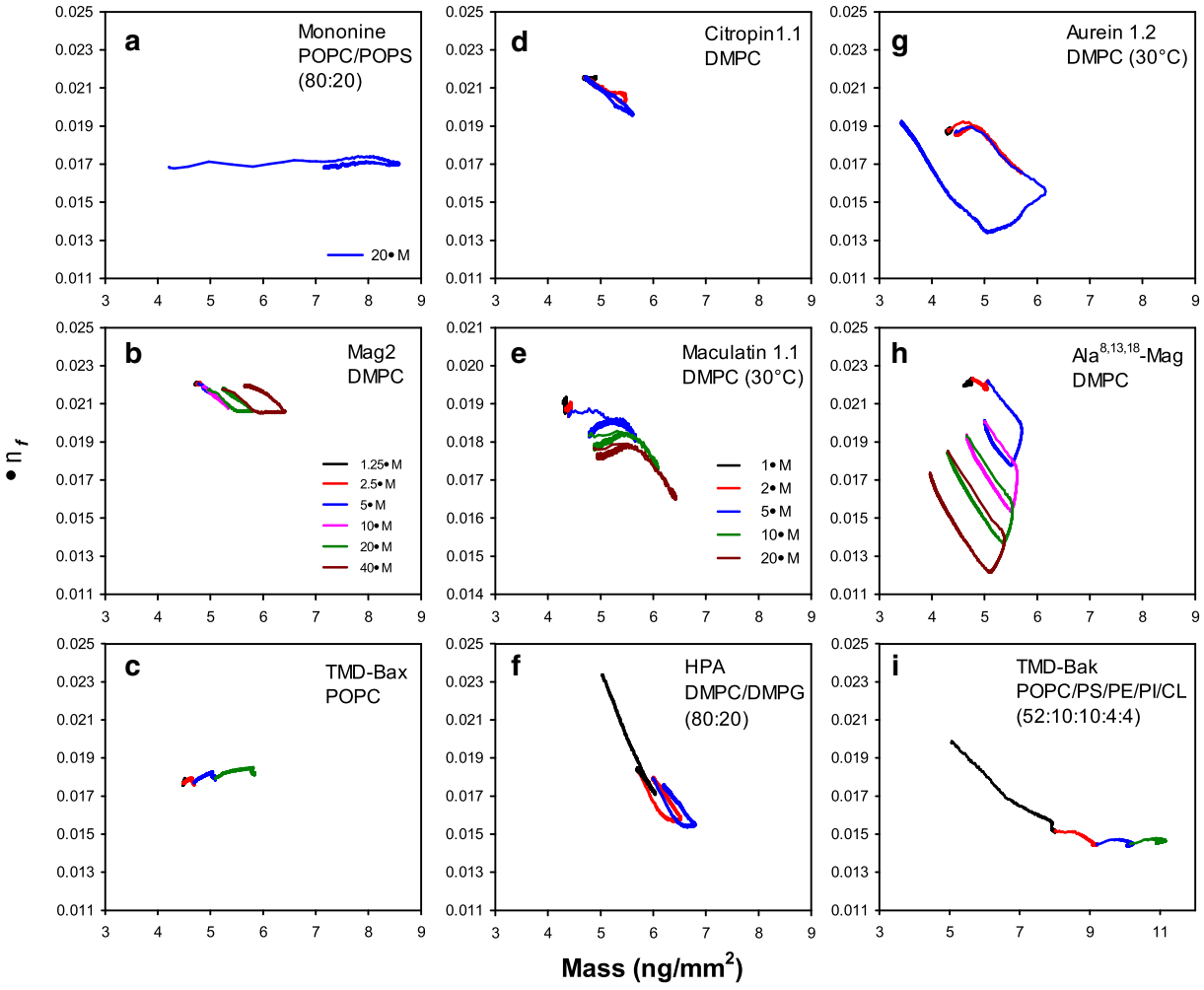

Fig. 3. Analysis of changes in bilayer order (as measured by the birefringence, Δn_f) as a function of membrane-bound peptide mass (m_p) allows the impact of peptide binding on the membrane structure to be determined for various sequential steps corresponding to surface binding, partial-full insertion, membrane expansion and membrane lysis, whereby decreases in Δn_f correspond to disordering in membrane structure. (a) binding of human blood coagulation factor, mononine, to the supported POPC/POPS (80:20) bilayer showed a large amount of protein mass bound to the membrane without significant changes in birefringence; (b) magainin2 induces disorder in DMPC bilayer above a threshold concentration and this disorder is fully reversible after peptide dissociation; (c) the accumulative binding of a peptide corresponding to the transmembrane domain of Bax protein to POPC showed increases in mass with little increase in POPC order. (d, e) The insertion of citropin1.1 and maculatin1.1 to DMPC bilayer showed no changes in bilayer order at low peptide concentration whilst significant disorder in bilayer were determined as peptide concentration increased. In contrast, (f) the insertion of HPA peptide into DMPC/DMPG (80:20) induced significant irreversible bilayer disorder with a low membrane-bound peptide mass. (g) The lysis of DMPC membrane by aurein1.2 showed multiple sequential changes in bilayer disorder where the birefringence returned to the starting value with significant loss in overall mass; whilst (f) binding of maginin 2 analogue ($Ala^{8,13,18}$-mag) to DMPC showed significant mass loss with irreversible bilayer disordering as a result of bilayer expansion. (i) Binding of a peptide corresponding to the transmembrane domain of Bak protein to a mitochondrial membrane mimic (POPC/PS/PE/PI/CL = 52:10:10:4:4) showed significant irreversible bilayer disordering with increasing membrane-bound peptide mass. (Compiled from references [12,72–74,78,93,99]).

surface [100]. DPI measurements of mass, thickness and density allowed the very early stages of Aβ40 and Aβ42 aggregation to be measured. The initiation of aggregation was accompanied by a decrease in density without significant changes in thickness whilst during the elongation and higher order aggregate an abrupt increase in thickness was obtained [100].

Membranes play an important role in mediation of the conformational changes, initiation of low molecular weight oligomers, nucleation of mature fibrils and alteration of structural morphology with specific pathological features. Studying the time-resolved formation of peptide and protein aggregates on a membrane template will help to understand the factors involved in initiating and modulating aggregation and the arrest of fibril formation by inhibitors of aggregation. SPR-based techniques have been used to study the membrane interaction of amyloidogenic molecules [101]. However, waveguide-based optical sensors have been employed to simultaneously characterise the binding kinetics and structural changes during the association of aggregated species in supported membrane systems. The changes in the optical properties of the membranes that occur during the process of time-dependent peptides/proteins aggregations have been shown for Aβ40 [102], prion proteins [92] and α-synuclein [76].

The role of raft domains in model neuronal membranes on the behaviour of raft-dependent Aβ aggregation has been characterised by the spectral shift of *s*- and *p*-polarisation obtained with PWR spectroscopy [102]. Aβ40 peptides bind to all model membranes composed of DOPC, sphingomyelin (SM), SM/Chol, DOPC/SM/Chol whilst only aggregates bind in the presence of SM. With the presence of cholesterol in the SM bilayers, a 5-fold stronger binding than to DOPC and SM-only bilayers was accompanied by a mass loss attributed to the removal of lipid molecules from the bilayer and transfer to the Gibbs border, which occurs upon peptide insertion into the bilayer and aggregation leading to lipid displacement. The ability of Aβ to preferentially bind and insert into the densely packed thicker SM microdomain over the less-ordered thinner DOPC domain was characterised as a biphasic binding process on the DOPC/SM/Chol ternary lipid bilayers. A transition from an initial positive spectral shift to a negative spectral shift with increasing membrane-bound peptide mass allowed the process of binding, insertion and bilayer expansion to be observed for Aβ aggregation on

membranes. In addition to characterising the mass changes, the changes in the optical properties (RI and thickness) of lipid bilayers during the process of Aβ binding and aggregation were quantitatively characterised by spectral simulation of the experimental spectral parameters, which provided further understanding of the effect of amyloid aggregation on membrane perturbation. No change in the bilayer properties was observed during the initial Aβ binding to the bilayer surface of DOPC and SM, whilst a large decrease in the RI was observed for the cholesterol-containing bilayers, which facilitated the insertion and aggregation of Aβ involving bilayer reorganisation. PWR analysis combined with liposome dye-release and cryo-TEM of the binding of various Aβ1–42 variants to DOPG bilayers showed the effect of oligomeric aβ1–42 on membrane perturbation and cell toxicity [103].

PWR has also provided insight into the changes in the mass density and structural ordering of the amyloid-membrane complex [51,104]. Whilst the interaction of non-toxic (WT) and toxic HET-s prion peptides with asolectin, DOPC and DPPG membranes showed increases in the resonance angle position, the role of lipids in mediating the binding and aggregation of HET-s could be further differentiated by resolving the magnitude if the angle shift, the rate of binding and the extent of the membrane reorganisation. Larger spectral shifts were observed for peptides binding to the negatively charged DOPG membranes indicating the importance of electrostatic interactions in promoting peptide accumulation. In addition, an increase in membrane thickness of 3 nm was observed for binding of the non-toxic and toxic HET-s prion to the DOPG bilayer. In contrast, the splitting of the resonance minimum of the s-polarisation data was related to the formation of microdomains for different organisations of bound peptide. The interaction of toxic protein with DOPG formed three domains with different thicknesses; 60% of the membrane area showed no change in thickness whilst 25% showed an increase of 6 nm and 15% showed an increase thickness of 10 nm upon binding of the toxic prion aggregate. However, no significant difference was observed for the binding kinetics of either the toxic or non-toxic prion aggregate. Thus, lateral membrane reorganisation of different microdomains with different optical properties can be measured as splitting in the resonance spectra. However, unlike ligand–receptor interactions, the affinity constants for amyloid–membrane interactions cannot be accurately determined for the complex coherent changes associated with peptide–lipid interactions, membrane reorganisation and protein self-assembly.

The changes in the optogeometrical properties for the binding and during the process of amyloid formation on the membrane have also been characterised for the prion proteins [92] and α-synuclein using DPI which provide insight into early events in the aggregation [76]. Based on the DPI phase shift data, the extent of aggregation was significantly enhanced by the electrostatic interaction between the positively charged PrP peptide and negatively charged POPS lipid bilayer resulting in a thicker and more densely packed protein layer compared to those on POPC bilayers. In addition, further growth of the protein aggregate layer, as indicated by increases in both TM and TE phases, was observed upon incubation of PrP on POPC/POPS bilayer.

The role of lipid composition on α-synuclein aggregation and the impact of aggregation on bilayer properties were also characterised by the changes of the optical properties in SLBs and liposomes tethered on DPI chip surfaces [76]. Strong binding was mediated by the electrostatic interaction with the DOPS-containing bilayers. α-Synuclein binding was further enhanced by increasing the DOPE content in the membranes. By following the variations in mass and birefringence upon α-synuclein binding, the protein–lipid stoichiometry for these changes in the optical properties of bilayers was correlated with the mode of interaction. Two processes for α-synuclein binding to different SLBs except DOPC suggested the initial binding caused membrane expansion as a result of insertion followed by a second stage of surface binding without a change in bilayer order. The bilayer disorder induced by α-synuclein showed a low degree of reversibility after rinsing. By comparing the optical properties of SLBs and tethered liposomes, a membrane remodelling mechanism was proposed for the α-synuclein–membrane interaction, in contrast to the transmembrane insertion adopted by AMPs. Specifically, α-synuclein binding to membranes involved insertion at the head group region leading to lateral expansion of lipids. The partial insertion was then facilitated and enhanced by defects in lipid packing and the expansion of lipid resulted in the membrane remodelling and thinning.

Overall, the amyloid layer may be anisotropic and its formation onto an existing anisotropic layer may modulate the overall birefringence. However, the formation of the anisotropic peptide assembly may also induce disordering in the bilayer. In addition, amyloid formation is a kinetic process and the molecular mechanism of amyloid deposition may follow a wide range of pathways which may include rod-like assembly formation in addition to sheets, spheroids etc. Therefore, new techniques are required to resolve the birefringence changes associated with these systems.

Table 2
Molar ratio of peptide to lipid determined at the point where mass loss and membrane disruption.

	DMPC	DMPC/DMPG (4:1)
Aurein 1.2	1:14	1:23
Magainin 2	–	1:15
$Ala^{8,13,18}$-Magainin 2	1:8	1:13

5.3. Apoptotic peptides

Mitochondrial outer membrane permeabilization (MOMP) is considered the initial step in intrinsic apoptosis with the formation of the apoptotic pore, which has been related to the release of pro-apoptotic mitochondrial resident proteins including cytochrome c (cyt c) and smac/diablo to the cytosol and subsequent activation of caspases. The function of the Bcl-2 proteins in apoptosis has been linked to their direct interaction with the mitochondrial membrane leading to MOMP. In recent years the role of lipids in the Bcl-2 regulated apoptotic pathway has been recognised and is central to the "embedded together" model [105–107]. This draws together aspects of both direct and indirect activation but also takes into account the importance of mitochondrial membranes in facilitating key interactions such as those involved in the activation of Bax by the BH3-only protein tBid, and the inhibition of Bax oligomerisation by the anti-apoptotic family members. The precise role of the membrane in these interactions, however, is still unclear. More specifically, an understanding of the functional role of Bcl-2 protein secondary structure variation caused by protein–membrane interactions and its effect on relative membrane affinity and disorder will be central to understanding the events that lead to MOMP.

Recent studies in this area seek to further our understanding of the mechanism by which the Bcl-2 proteins interact with the mitochondrial and plasma membranes, and in turn how these membranes are restructured upon protein contact. A membrane perturbation study based on the birefringence analysis has been focused particularly on the hydrophobic C-terminal trans-membrane domain (TMD) of Bcl-2 proteins interacting with membrane mimics including plasma membrane, mitochondrial outer membrane and mitochondrial outer membrane with cardiolipin (Fig. 5) [93]. Bcl-2 related peptides bind selectively to mitochondrial mimics over plasma membrane mimics and that anti-apoptotic peptides exert a different effect on the bilayer to pro-apoptotic peptides (Fig. 5). Most significantly membrane binding behaviour of transmembrane domain-derived synthetic peptides indicate an activity-based classification of these peptides in which there is a clear correlation between the membrane disruptive properties and the biological activity [93]. The TMD peptides preferentially bound to mitochondrial membranes that in turn induce conformational changes in the peptides. The TMD peptides did not perturb plasma membranes and were therefore non-toxic to cells, however

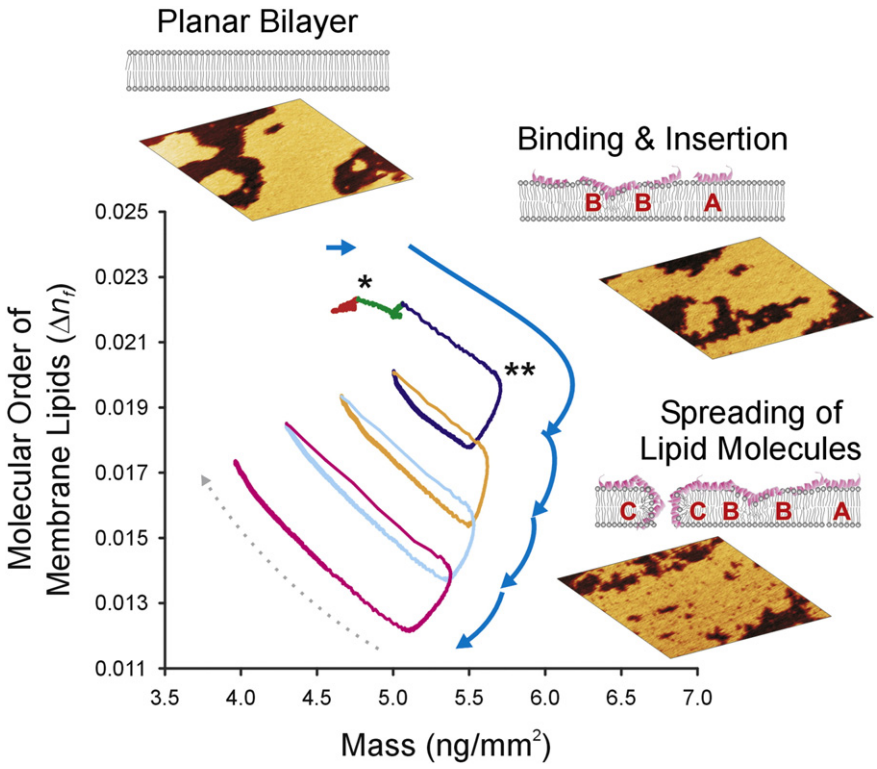

Fig. 4. The changes in the molecular order of supported DMPC bilayers induced by the alanine substituted magainin 2 ($Ala^{8,13,18}$-mag2) showed a multi-stage process of membrane destabilisation with increases in membrane-bound peptide mass. The extent of bilayer disordering from binding leading to membrane expansion correlated well with the sequential changes of spreading of lipid molecules on the solid support bilayer imaged in real-time by AFM. The peptide induced membrane expansion involves the interconversion of multiple conformation states (A, B and C) of the peptide–lipid complexes. The peptides were injected consecutively onto the DMPC bilayer from 1.25 to 40 μM with a 2-fold increment in concentration. The association and dissociation of $Ala^{8,13,18}$-mag2 are denoted by the solid arrow and dotted line, respectively. * corresponds to the initial membrane disordering and ** corresponds to the onset of membrane disruption with mass loss. (Adapted from [74]).

when the peptides were artificially introduced into cells they targeted mitochondria inducing MOMP and caused cell death (Fig. 5). Importantly, at sub-lethal doses, the TMD peptides exerted a mitochondrial priming activity that enhances the cell death-inducing properties of the chemotherapeutic drug cisplatin. These results clearly show that, even the examination of isolated transmembrane domain can provide significant insight into the role of the mitochondrial Bcl-2 protein recruitment. In particular, the ability to measure comparative changes in membrane structure of a model plasma membrane and mitochondrial membrane by DPI has provided significant new insight into the mechanism of apoptoptic pore formation by Bcl proteins. These studies also lay the foundation for understanding selectivity of Bcl proteins for mitochondrial membrane relative to the plasma membrane and the role of this selectivity in apoptosis and development of cancer therapeutics.

6. Kinetic analysis of experimental data to define binding mechanisms

Most studies of membrane-active peptides have focused on the overall mechanism—either in terms of the actual efficacy of the peptide such as cell lysis and cargo transport or the final end-point of mechanisms such as pore formation or micellisation. However, in order to fully understand the mechanism of action of the peptides, it is important to characterise the sequence of events involved in the entire dynamic process. For example, a peptide may bind the membrane, reorient with different topology, insert further into the membrane, destabilise the membrane, and then interact with other peptides to form pores or other structural assemblies. Much research limits itself to either the initial peptide binding step with respect to the surface charges or the formation of the final structure of the lipid–peptide complex, neglecting the intermediate steps. However, these intermediate steps may well be critical for the peptide to achieve its function, and understanding these steps may lead to new opportunities for peptide design in therapeutics. The question that must be asked is not merely what overall mechanism(s) are involved, but what the intermediate steps are, and what factors may affect the sequence of transitions that lead to the ultimate activity of the peptide. Determining the intermediate states requires a thorough characterisation of peptide and membrane structural changes and the kinetics associated with different intermediate steps. This information is now emerging with optical waveguide technologies through kinetic analysis of real-time binding data using specific kinetic models and will enable the design of peptides to modulate their activity resulting in more powerful and flexible use for mechanistic understanding of biomolecular membrane interactions.

6.1. Kinetic models

Kinetic models, with regard to peptide–membrane interactions, are an approximate mathematical representation of the process by which a peptide will bind to the membrane. A simple example of such a model is the *one-state* model (sometimes called "Langmuir binding") in which the peptide binds and dissociates with the membrane at concentration-dependent rates [29]. The peptide does not change state at the membrane, and there is only one way in which it may bind. This may be represented by the reaction:

$$P + L \leftrightarrow PL$$

where P represents the peptide free in solution, L represents the unbound lipid membrane, and PL represents the complex formed by the binding of the peptide to the membrane. Kinetic models are modelled

using a system of differential equations describing the rate of change of various states in substances, in this case the reaction is defined by the equation:

$$dM/dt = k_{a1}C_P M_{max} - (k_a C_P + k_d)M$$

However it has been found that this model provides an inadequate representation of binding processes [108], and more sophisticated models must be used. A more complex model is the *two-state* model [108], so called because the peptide forms one state on initial binding to the membrane, and then undergoes a transition to a second state once it is bound. This may be represented by the reaction:

$$P + L \leftrightarrow PL_1 \leftrightarrow PL_2$$

and mathematically by the system of differential equations

$$dM_1/dt = k_{a1}C_P(M_{max} - M_1 - M_2) - k_{d1}M_1 - k_{a2}M_1 + k_{d2}M_2$$
$$dM_2/dt = k_{a2}M_1 - k_{d2}M_2$$

Further elaborations upon this model are possible; the *three-state* model [108] is the logical extension where the bound peptide, already in its second bound state, may undergo a transition to a third state. *Parallel reactions* models involve simultaneous reactions. In a simple case this may involve two one-state reactions; in more complex cases some or all reactions may have multiple states. Also, in any of above described models, there may be co-operativity in the reactions, i.e. interactions between peptides on the surface may speed up the transition from one state to another.

The three-state model, which will be discussed extensively in the next section, is represented by the equations

$$dM_1/dt = k_{a1}C_P(M_{max} - M_1 - M_2) - k_{d1}M_1 - k_{a2}M_1 + k_{d2}M_2$$
$$dM_2/dt = k_{a2}M_1 - k_{d2}M_2 - k_{a3}M_2 + k_{d3}M_3$$
$$dM_3/dt = k_{a3}M_2 - k_{d3}M_3$$

6.2. Incorporation of birefringence into kinetic models

The models described above are typically used in kinetic modelling with only one dependent variable, mass. This restricts the ability to differentiate between the more complex models, as shown by the binding of the antimicrobial peptide HPA3 to the unsaturated zwitterionic bilayer POPC (Fig. 6) [108]. Assuming no structural changes in the membrane using only the mass, the process can be very well fit by the two-state model, and the three-state model only provides a very slight improvement to the fit. From this, one might conclude that there are only two significant states involved in the binding of this peptide. However, when considering the membrane structural changes, the measurements of membrane order, represented by birefringence, are now also included in the analysis. This is based on the assumptions that peptide bound to the membrane changes the birefringence of the membrane, and that the change in birefringence is linearly proportional to the change in mass. However, different states of the peptide may have different levels of impact on the membrane; for example, a peptide bound to the surface may only have a small impact on birefringence, whilst the same peptide when fully inserted may have a much larger impact. This is mathematically modelled with the following algebraic equations that link the birefringence to the mass of peptide in its states.

For the *two-state* model:

$$n_f = n_1 M_1 + n_2 M_2$$

For the *three-state* model:

$$n_f = n_1 M_1 + n_2 M_2 + n_3 M_3$$

Where n_1, n_2, n_3 are constants specific to the interaction taking place.

These models have been applied to binding mechanism of the peptide HPA3 [108]. By fitting these parameters to the model it becomes clear that the *two-state* model is inadequate for the above reaction, as it gives a poor fit and does not account for the characteristics of the binding curve (Fig. 6). However, using a *three-state* model provides a much better fit, including the notable downward kink in the final stages (Fig. 6). This shows that simultaneously measure both mass and birefringence, additional steps in the binding process may be revealed that previous technologies measuring the mass-only changes could not have shown. In contrast, there was only a slight improvement in the fit to the binding profiles of HPA3 to the saturated DMPC bilayer below the transition temperature when using the *three-state* model. The *two-state* model already gave a good fit suggesting that there are only two significant states that impact on mass or birefringence [29].

This analysis allowed the calculation of the normal association and dissociation constants as frequently described in kinetic analysis, but in addition, it also determines additional membrane disordering parameters that quantify the birefringence–mass relationship for each state of the reaction, with larger numbers indicating a greater impact on membrane structure per unit of peptide in that particular state. For example,

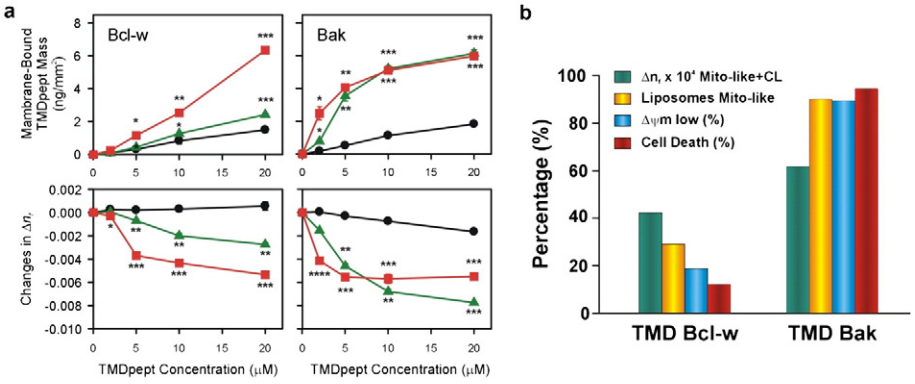

Fig. 5. The membrane binding properties of peptides corresponding to the transmembrane domain peptides (TMDpept) of Bcl-2 family members were assessed by the changes in bilayer order as a function of membrane-bound peptide mass using DPI. (a) For both Bcl-w and Bak peptides binding to POPC (Black Line), a plasma membrane-like model, there is little change in bilayer order measured by birefringence (Δn_f). In contrast to the Bcl-w TMD peptide, TMD-Bak induced significant bilayer perturbation of the Mito-like membrane (Green Line) and a lower TMDpept concentration was required to induce significant perturbations to the cardiolipin-containing Mito-like membranes (Red Line). (b) The results showed a good correlation between the bilayer perturbation (Δn_f) of Mito-like membrane, calcein release induced by TMDpepts and the loss of the membrane potential of isolated mitochondrial and the cell viability. (Adapted from [93]).

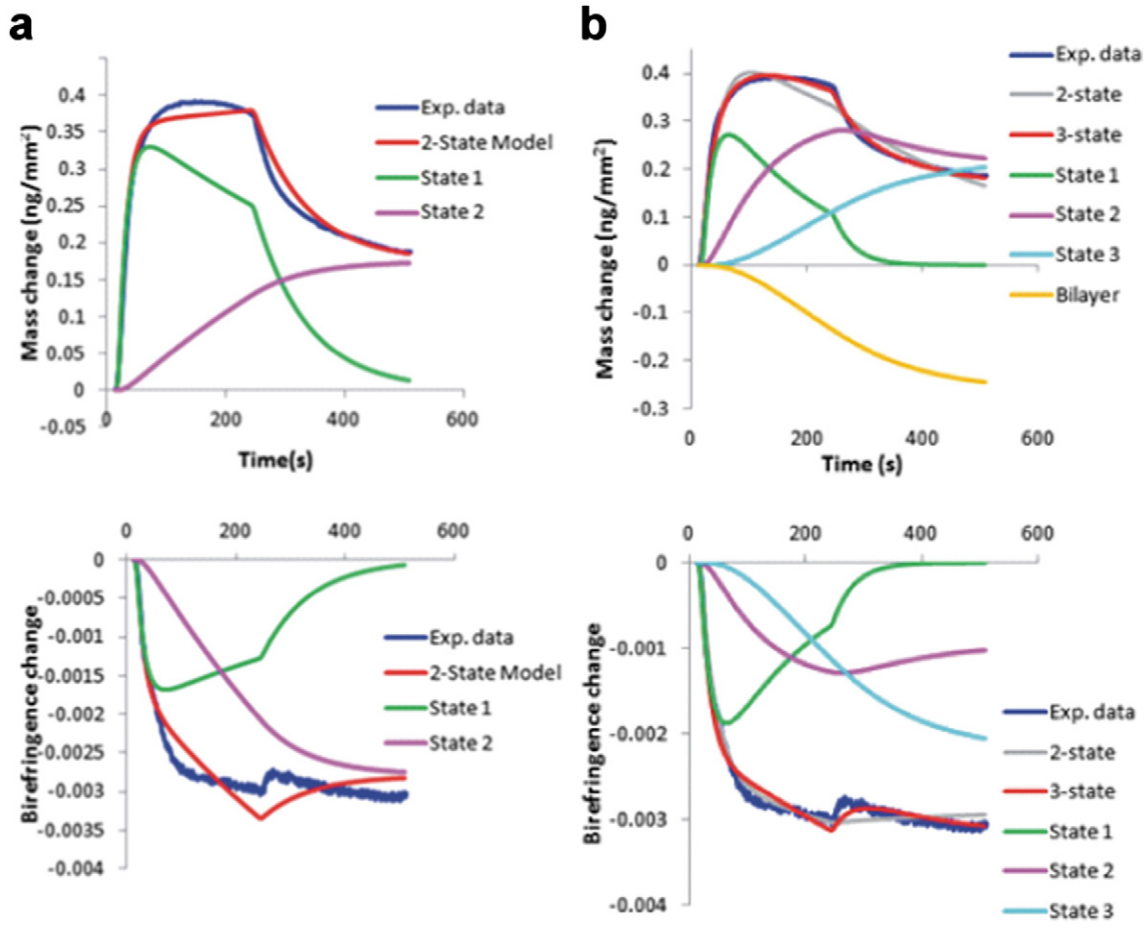

Fig. 6. The binding of HPA3 to supported DMPC bilayer analysed by a two-state and a three-state binding model showing the relative proportions of the peptide in each state according to the parameters of the model. The three-state fitting programme can deconvolute both mass changes and bilayer disordering into sequential steps of peptide insertion into membrane involving the component of bilayer expansion. However, the two-state model poorly fit the binding and changes in bilayer order. (Adapted from [108]).

the membrane disordering parameters for HPA3 on POPC calculated using a three-state model are −0.0048 for state 1, −0.0042 for state 2, and a much larger value −0.0274 for state 3. From this it can be seen that whilst the first two states had a similar impact on the membrane birefringence, the third state had a much larger effect [108].

The results of the model can easily be graphed to visualise the proportions of peptide in various states as the dynamic changes in membrane progress and is shown for HPA3 on POPC in Fig. 6. Here it can be seen that the amount of peptide in State 1 rises very rapidly at the start of the injection, but then falls away gradually as it progressively converts to State 2. Once the injection is complete the peptide in State 1 rapidly dissociates, but the peptide in State 2 remains bound and gradually converts to State 3 [108]. This approach has also been recently applied to the analysis of the intracellular Helix 8 of the angiotensin II type 1A receptor and has highlighted a significant role of phosphatidylinositols in the regulation of this receptor during signalling [109].

7. Membrane ordering profiles: new insight into biological processes

Membrane bilayer components alter the physiological profiles of a vast number of membrane proteins, either through specific interactions with the protein itself or alteration of membrane physical properties such as curvature, lateral pressure, and bilayer thickness [1,5]. For a large number of cases, the available evidence points to a clear link between peptide/protein structure/function, and the surrounding membrane composition. For example, as discussed above, antimicrobial peptide action is controlled by the nature of the bacterial and mammalian membrane [110], that the apoptotic cascade involving the Bcl-2 family of proteins is mediated by mitochondrial membrane properties [107] and that amyloid formation is induced and modulated by membrane binding [111].

The data that is now available from techniques such as DPI provides the opportunity to categorise membrane-mediated events in terms of patterns of membrane structure changes. In particular mass–birefringence plots, which reveal the changes in membrane ordering that occur during peptide binding, now allow very detailed and subtle differences in the interactions between lipids and peptides to be visualised. This birefringence analysis provides novel information on the impact of peptides on the changes in organisation occurring within a lipid bilayer, and assists in describing the behaviour of membrane-active peptides when interacting with a lipid membrane. Overall a number of transitions can be described based on the birefringence vs. mass plots (as illustrated in Fig. 7), which can be used to evaluate peptide behaviour and mechanism of action and are the centrepiece of this new membrane biophysical methodology. The molecular events corresponding to these four transitions are schematically drawn in Fig. 7 [12,72–74,99]. Compared to reasonably similar overall profiles obtained by SPR, the wide variety of membrane structure changes evident by DPI could not be anticipated and has opened up exciting opportunities for more detailed understanding of a vast range of membrane-mediated biological events. The examples described above demonstrate how knowledge of the membrane structure changes significantly informs our understanding of a wide range of biological processes.

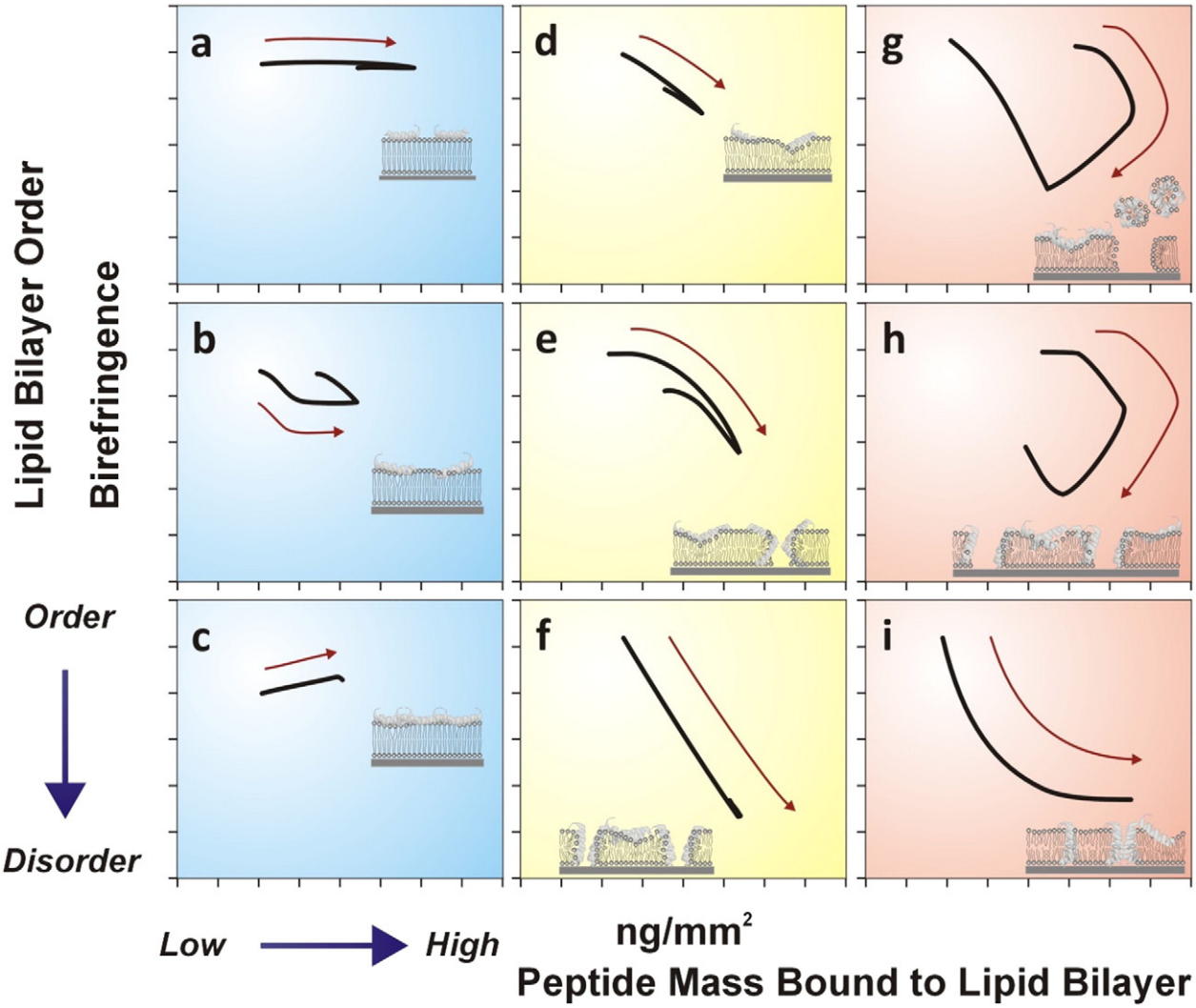

Fig. 7. The molecular mechanism of membrane disruption consists of a series of intermediate states, each representing an ensemble of closely-related bilayer structures. For the examples of antimicrobial peptides and apoptotic peptides induced bilayer disordering, three general membrane-inserted states are defined corresponding to (1) surface parallel-bound state (a–c), (2) partially inserted state (d–f) and (3) significantly inserted state with membrane lysis or expansion (g–i).

Based on the multiple stages of membrane structure changes evident in Fig. 3, new models can be defined for the molecular mechanism of action in terms of a series of intermediate states, each representing an ensemble of closely-related bilayer structures, such as depicted schematically in Fig. 7 for antimicrobial peptides and apoptotic peptides. In this example, three general membrane-inserted states are outlined corresponding to (1) surface-bound peptides (Fig. 7a–c), (2) partially inserted peptides (Fig. 7d–f) and (3) significantly inserted peptides (Fig. 7g–i). This model also describes alternate pathways of intermediate membrane states that occur in the presence of increasing amounts of bound peptide; the prevalence of each state is dependent on the peptide and the lipid composition. This model, based on birefringence changes at critical mass loadings, allows the properties of membrane-active peptides to be analysed in terms of surface binding, insertion, membrane opening and bilayer lysis, and in more detail than has been previously possible in terms of dynamic structural changes. In particular, the molecular events prior to membrane lysis can be fully characterised in terms of bilayer structural changes and provides new criteria that can guide the design of selective antibacterial peptides.

8. Final considerations and future directions

The knowledge of structural changes associated with biomolecular interactions underpins the definition of a molecular mechanism. For membrane structure changes, we conventionally require multiple techniques to develop a picture of membrane interactions of any particular class of peptides/protein. The optical biosensors described in this review now allow rapid measurement and definition of membrane structure change, recovery and repair of any membrane–peptide/protein set or interacting partners.

These and many other examples clearly demonstrate that the membrane bilayer is an active participant in an enormous number of biological processes. However, despite these established paradigms, the complete lack of molecular details of the changes in membrane structure during the binding and action of a peptide or protein is severely restricting new progress, firstly in defining these biological processes in the detail required to fully understand the mechanism, and secondly to exploit this understanding in the design of new therapeutics to modulate these processes where their dysregulation underpins disease.

Although the membrane bilayer shares a close relationship with complex biological processes, the 'how', 'when' and 'why' of this relationship remains less clear and, if we are to fully understand these systems, the membrane must be a strong focus of future studies. Determining how these concepts apply to other systems will only be achieved through detailed investigations on membrane structures, which until now have been severely hampered by the lack of techniques to readily measure membrane structure changes in real-time. DPI (Fig. 1c) now makes membrane structure analysis amenable to biophysical investigations, allowing us to characterise how the membrane controls the function of a number of biological systems through a systematic analysis of membrane structure. In addition, the complication of linear dichroism and birefringence of protein assembly such as the formation of rod-like amyloid on the anisotropic properties of lipid bilayer require more complex models to resolve the overall changes in birefringence for several distinctive layers.

Collectively, the techniques and results reviewed here demonstrate that this unprecedented knowledge of membrane structural change profiles provides significant new insights into membrane-mediated processes. Not only does this information provide a more detailed molecular understanding of these events, but knowledge of the structure changes associated with both the membrane as well as the interacting ligands will open up new avenues for therapeutic intervention.

In summary, this substantial amount of new information on membrane structure changes now sets the scene for a completely new approach to studying membrane-mediated biological systems. The unique advantage of DPI is that it allows real-time measurement of bilayer structure changes during peptide binding and results demonstrate that the mechanisms of bilayer disturbance differ significantly between different classes of peptides and proteins. The combination of DPI with other biophysical techniques now opens the door to redefining molecular mechanism of biomolecular interactions in which the membrane bilayer is a key player.

In this context the membrane–structure interaction profiles will form the basis of a membrane structure "atlas", analogous to the protein structure atlas which is the cornerstone of protein structure and function studies. This membrane–structure Atlas will not only provide a reference of membrane behaviour to allow comparison of new data with a data base of membrane profiles, but will lead to a new paradigm in the role of the membrane as an interactive partner in biology and reveal new approaches to therapeutic development.

Transparency document

The Transparency document associated with this article can be found, in the version.

Acknowledgements

The financial support of the National Health & Medical Research Council (#1044327) and the Australian Research Council (DP1110101866) is gratefully acknowledged.

References

[1] J.C. Holthuis, A.K. Menon, Lipid landscapes and pipelines in membrane homeostasis, Nature 510 (2014) 48–57.
[2] G. van Meer, Cellular lipidomics, EMBO J. 24 (2005) 3159–3165.
[3] G. van Meer, D.R. Voelker, G.W. Feigenson, Membrane lipids: where they are and how they behave, Nat. Rev. Mol. Cell Biol. 9 (2008) 112–124.
[4] Y.M. Zhang, C.O. Rock, Membrane lipid homeostasis in bacteria, Nat. Rev. Microbiol. 6 (2008) 222–233.
[5] A.I. de Kroon, P.J. Rijken, C.H. De Smet, Checks and balances in membrane phospholipid class and acyl chain homeostasis, the yeast perspective, Prog. Lipid Res. 52 (2013) 374–394.
[6] G. Di Paolo, P. De Camilli, Phosphoinositides in cell regulation and membrane dynamics, Nature 443 (2006) 651–657.
[7] M.R. Krause, S.L. Regen, The structural role of cholesterol in cell membranes: from condensed bilayers to lipid rafts, Acc. Chem. Res. 47 (2014) 3512–3521.
[8] J.P. Slotte, Biological functions of sphingomyelins, Prog. Lipid Res. 52 (2013) 424–437.
[9] C. Avitabile, L.D. D'Andrea, A. Romanelli, Circular dichroism studies on the interactions of antimicrobial peptides with bacterial cells, Sci. Rep. 4 (2014) 4293.
[10] K. Hall, M.I. Aguilar, Membrane interactions of antimicrobial beta-peptides: the role of amphipathicity versus secondary structure induction, Biopolymers 92 (2009) 554–564.
[11] E.C. McCusker, C. Bagneris, C.E. Naylor, A.R. Cole, N. D'Avanzo, C.G. Nichols, B.A. Wallace, Structure of a bacterial voltage-gated sodium channel pore reveals mechanisms of opening and closing, Nat. Commun. 3 (2012) 1102.
[12] D.I. Fernandez, T.H. Lee, M.A. Sani, M.I. Aguilar, F. Separovic, Proline facilitates membrane insertion of the antimicrobial peptide maculatin 1.1 via surface indentation and subsequent lipid disordering, Biophys. J. 104 (2013) 1495–1507.
[13] A. Ramamoorthy, D.K. Lee, J.S. Santos, K.A. Henzler-Wildman, Nitrogen-14 solid-state NMR spectroscopy of aligned phospholipid bilayers to probe peptide–lipid interaction and oligomerization of membrane associated peptides, J. Am. Chem. Soc. 130 (2008) 11023–11029.
[14] H. Yao, M. Hong, Conformation and lipid interaction of the fusion peptide of the paramyxovirus PIV5 in anionic and negative-curvature membranes from solid-state NMR, J. Am. Chem. Soc. 136 (2014) 2611–2624.
[15] Y. Shai, ATR–FTIR studies in pore forming and membrane induced fusion peptides, Biochim. Biophys. Acta 1828 (2013) 2306–2313.
[16] S.A. Tatulian, Structural characterization of membrane proteins and peptides by FTIR and ATR–FTIR spectroscopy, Methods Mol. Biol. 974 (2013) 177–218.
[17] D.I. Fernandez, A.P. Le Brun, T.H. Lee, P. Bansal, M.I. Aguilar, M. James, F. Separovic, Structural effects of the antimicrobial peptide maculatin 1.1 on supported lipid bilayers, Eur. Biophys. J. 42 (2013) 47–59.
[18] F. Heinrich, M. Losche, Zooming in on disordered systems: neutron reflection studies of proteins associated with fluid membranes, Biochim. Biophys. Acta 1838 (2014) 2341–2349.
[19] A.M. Whited, P.S. Park, Atomic force microscopy: a multifaceted tool to study membrane proteins and their interactions with ligands, Biochim. Biophys. Acta 1838 (2014) 56–68.
[20] M. Zocher, C.A. Bippes, C. Zhang, D.J. Muller, Single-molecule force spectroscopy of G-protein-coupled receptors, Chem. Soc. Rev. 42 (2013) 7801–7815.
[21] N. Buzhynskyy, M. Golczak, J. Lai-Kee-Him, O. Lambert, B. Tessier, C. Gounou, R. Berat, A. Simon, T. Granier, J.M. Chevalier, S. Mazeres, J. Bandorowicz-Pikula, S. Pikula, A.R. Brisson, Annexin-A6 presents two modes of association with phospholipid membranes. A combined QCM-D, AFM and cryo-TEM study, J. Struct. Biol. 168 (2009) 107–116.
[22] N.J. Cho, G. Wang, M. Edvardsson, J.S. Glenn, F. Hook, C.W. Frank, Alpha-helical peptide-induced vesicle rupture revealing new insight into the vesicle fusion process as monitored in situ by quartz crystal microbalance-dissipation and reflectometry, Anal. Chem. 81 (2009) 4752–4761.
[23] X.P. Xu, D. Zhai, E. Kim, M. Swift, J.C. Reed, N. Volkmann, D. Hanein, Three-dimensional structure of Bax-mediated pores in membrane bilayers, Cell Death Dis. 4 (2013) e683.
[24] E.C. Yan, L. Fu, Z. Wang, W. Liu, Biological macromolecules at interfaces probed by chiral vibrational sum frequency generation spectroscopy, Chem. Rev. 114 (2014) 8471–8498.
[25] S. Ye, K.T. Nguyen, S.V. Le Clair, Z. Chen, In situ molecular level studies on membrane related peptides and proteins in real time using sum frequency generation vibrational spectroscopy, J. Struct. Biol. 168 (2009) 61–77.
[26] J.R. Henriksen, T.L. Andresen, Thermodynamic profiling of peptide membrane interactions by isothermal titration calorimetry: a search for pores and micelles, Biophys. J. 101 (2011) 100–109.
[27] T. Wieprecht, O. Apostolov, M. Beyermann, J. Seelig, Membrane binding and pore formation of the antibacterial peptide PGLa: thermodynamic and mechanistic aspects, Biochemistry 39 (2000) 442–452.
[28] K. Hall, T.H. Lee, M.I. Aguilar, The role of electrostatic interactions in the membrane binding of melittin, J. Mol. Recognit. 24 (2011) 108–118.
[29] H. Mozsolits, M.I. Aguilar, Surface plasmon resonance spectroscopy: an emerging tool for the study of peptide–membrane interactions, Biopolymers 66 (2002) 3–18.
[30] N. Papo, Y. Shai, Exploring peptide membrane interaction using surface plasmon resonance: differentiation between pore formation versus membrane disruption by lytic peptides, Biochemistry 42 (2003) 458–466.
[31] J.J. Ramsden, Molecular orientation in lipid bilayers, Philos. Mag. B 79 (1999) 381–386.
[32] S. Singh, M. Kalle, P. Papareddy, A. Schmidtchen, M. Malmsten, Lipopolysaccharide interactions of C-terminal peptides from human thrombin, Biomacromolecules 14 (2013) 1482–1492.
[33] S. Singh, G. Kasetty, A. Schmidtchen, M. Malmsten, Membrane and lipopolysaccharide interactions of C-terminal peptides from S1 peptidases, Biochim. Biophys. Acta 1818 (2012) 2244–2251.
[34] J. Escorihuela, M.A. Gonzalez-Martinez, J.L. Lopez-Paz, R. Puchades, A. Maquieira, D. Gimenez-Romero, Dual-polarization interferometry: a novel technique to light up the nanomolecular world, Chem. Rev. 115 (2015) 265–294.
[35] P. Kozma, F. Kehl, E. Ehrentreich-Forster, C. Stamm, F.F. Bier, Integrated planar optical waveguide interferometer biosensors: a comparative review, Biosens. Bioelectron. 58 (2014) 287–307.
[36] Z. Salamon, S. Devanathan, G. Tollin, Plasmon-waveguide resonance spectroscopy studies of lateral segregation in solid-supported proteolipid bilayers, Methods Mol. Biol. 398 (2007) 159–178.
[37] J. Voros, J.J. Ramsden, G. Csucs, I. Szendro, S.M. De Paul, M. Textor, N.D. Spencer, Optical grating coupler biosensors, Biomaterials 23 (2002) 3699–3710.
[38] X. Fan, I.M. White, S.I. Shopova, H. Zhu, J.D. Suter, Y. Sun, Sensitive optical biosensors for unlabeled targets: a review, Anal. Chim. Acta 620 (2008) 8–26.

[39] S.G. Patching, Surface plasmon resonance spectroscopy for characterisation of membrane protein–ligand interactions and its potential for drug discovery, Biochim. Biophys. Acta 1838 (2014) 43–55.
[40] T.H. Lee, H. Mozsolits, M.I. Aguilar, Measurement of the affinity of melittin for zwitterionic and anionic membranes using immobilized lipid biosensors, J. Pept. Res. 58 (2001) 464–476.
[41] I. Szekacs, N. Kaszas, P. Grof, K. Erdelyi, I. Szendro, B. Mihalik, A. Pataki, F.A. Antoni, E. Madarasz, Optical waveguide lightmode spectroscopic techniques for investigating membrane-bound ion channel activities, PLoS One 8 (2013) e81398.
[42] G. Tollin, Z. Salamon, V.J. Hruby, Techniques: plasmon-waveguide resonance (PWR) spectroscopy as a tool to study ligand–GPCR interactions, Trends Pharmacol. Sci. 24 (2003) 655–659.
[43] I.D. Alves, C.K. Park, V.J. Hruby, Plasmon resonance methods in GPCR signaling and other membrane events, Curr. Protein Pept. Sci. 6 (2005) 293–312.
[44] S. Devanathan, Z. Yao, Z. Salamon, B. Kobilka, G. Tollin, Plasmon-waveguide resonance studies of ligand binding to the human beta 2-adrenergic receptor, Biochemistry 43 (2004) 3280–3288.
[45] G.H. Cross, A.A. Reeves, S. Brand, J.F. Popplewell, L.L. Peel, M.J. Swann, N.J. Freeman, A new quantitative optical biosensor for protein characterisation, Biosens. Bioelectron. 19 (2003) 383–390.
[46] M.J. Swann, L.L. Peel, S. Carrington, N.J. Freeman, Dual-polarization interferometry: an analytical technique to measure changes in protein structure in real time, to determine the stoichiometry of binding events, and to differentiate between specific and nonspecific interactions, Anal. Biochem. 329 (2004) 190–198.
[47] H.G. Tompkins, E.A. Irene (Eds.), Handbook of ellipsometry *William Andrew Publishing*, Springer, 2005.
[48] Z. Salamon, H.A. Macleod, G. Tollin, Coupled plasmon-waveguide resonators: a new spectroscopic tool for probing proteolipid film structure and properties, Biophys. J. 73 (1997) 2791–2797.
[49] Z. Salamon, S. Devanathan, I.D. Alves, G. Tollin, Plasmon-waveguide resonance studies of lateral segregation of lipids and proteins into microdomains (rafts) in solid-supported bilayers, J. Biol. Chem. 280 (2005) 11175–11184.
[50] Z. Salamon, G. Tollin, Optical anisotropy in lipid bilayer membranes: coupled plasmon-waveguide resonance measurements of molecular orientation, polarizability, and shape, Biophys. J. 80 (2001) 1557–1567.
[51] E. Harte, N. Maalouli, A. Shalabney, E. Texier, K. Berthelot, S. Lecomte, I.D. Alves, Probing the kinetics of lipid membrane formation and the interaction of a nontoxic and a toxic amyloid with plasmon waveguide resonance, Chem. Commun. (Camb.) 50 (2014) 4168–4171.
[52] I.D. Alves, K.A. Ciano, V. Boguslavski, E. Varga, Z. Salamon, H.I. Yamamura, V.J. Hruby, G. Tollin, Selectivity, cooperativity, and reciprocity in the interactions between the delta-opioid receptor, its ligands, and G-proteins, J. Biol. Chem. 279 (2004) 44673–44682.
[53] I.D. Alves, S.M. Cowell, Z. Salamon, S. Devanathan, G. Tollin, V.J. Hruby, Different structural states of the proteolipid membrane are produced by ligand binding to the human delta-opioid receptor as shown by plasmon-waveguide resonance spectroscopy, Mol. Pharmacol. 65 (2004) 1248–1257.
[54] I.D. Alves, Z. Salamon, E. Varga, H.I. Yamamura, G. Tollin, V.J. Hruby, Direct observation of G-protein binding to the human delta-opioid receptor using plasmon-waveguide resonance spectroscopy, J. Biol. Chem. 278 (2003) 48890–48897.
[55] T. Georgieva, S. Devanathan, D. Stropova, C.K. Park, Z. Salamon, G. Tollin, V.J. Hruby, W.R. Roeske, H.I. Yamamura, E. Varga, Unique agonist-bound cannabinoid CB1 receptor conformations indicate agonist specificity in signaling, Eur. J. Pharmacol. 581 (2008) 19–29.
[56] Z. Salamon, S. Cowell, E. Varga, H.I. Yamamura, V.J. Hruby, G. Tollin, Plasmon resonance studies of agonist/antagonist binding to the human delta-opioid receptor: new structural insights into receptor–ligand interactions, Biophys. J. 79 (2000) 2463–2474.
[57] I.D. Alves, Z. Salamon, V.J. Hruby, G. Tollin, Ligand modulation of lateral segregation of a G-protein-coupled receptor into lipid microdomains in sphingomyelin/phosphatidylcholine solid-supported bilayers, Biochemistry 44 (2005) 9168–9178.
[58] I.D. Alves, I. Correia, C.Y. Jiao, E. Sachon, S. Sagan, S. Lavielle, G. Tollin, G. Chassaing, The interaction of cell-penetrating peptides with lipid model systems and subsequent lipid reorganization: thermodynamic and structural characterization, J. Pept. Sci. 15 (2009) 200–209.
[59] M.L. Jobin, P. Bonnafous, H. Temsamani, F. Dole, A. Grelard, E.J. Dufourc, I.D. Alves, The enhanced membrane interaction and perturbation of a cell penetrating peptide in the presence of anionic lipids: toward an understanding of its selectivity for cancer cells, Biochim. Biophys. Acta 1828 (2013) 1457–1470.
[60] Z. Salamon, G. Tollin, Graphical analysis of mass and anisotropy changes observed by plasmon-waveguide resonance spectroscopy can provide useful insights into membrane protein function, Biophys. J. 86 (2004) 2508–2516.
[61] I.D. Alves, C. Bechara, A. Walrant, Y. Zaltsman, C.Y. Jiao, S. Sagan, Relationships between membrane binding, affinity and cell internalization efficacy of a cell-penetrating peptide: penetratin as a case study, PLoS One 6 (2011) e24096.
[62] Z. Salamon, G. Lindblom, G. Tollin, Plasmon-waveguide resonance and impedance spectroscopy studies of the interaction between penetratin and supported lipid bilayer membranes, Biophys. J. 2003 (1796–1807) 84.
[63] R. Horvath, G. Fricsovszky, E. Papp, Application of the optical waveguide lightmode spectroscopy to monitor lipid bilayer phase transition, Biosens. Bioelectron. 18 (2003) 415–428.
[64] R.N. Lewis, Y.P. Zhang, R.N. McElhaney, Calorimetric and spectroscopic studies of the phase behavior and organization of lipid bilayer model membranes composed of binary mixtures of dimyristoylphosphatidylcholine and dimyristoylphosphatidylglycerol, Biochim. Biophys. Acta 1668 (2005) 203–214.
[65] S. Mabrey, J.M. Sturtevant, Investigation of phase transitions of lipids and lipid mixtures by sensitivity differential scanning calorimetry, Proc. Natl. Acad. Sci. U. S. A. 73 (1976) 3862–3866.
[66] J.J. Ramsden, Partition coefficients of drugs in bilayer lipid membranes, Experientia 49 (1993) 688–692.
[67] J.J. Ramsden, A dosimeter for oligopeptide hormones, Sensors Actuators B Chem. 30 (1996) 107–110.
[68] J.J. Ramsden, P. Schneider, Membrane insertion and antibody recognition of a glycosylphosphatidylinositol-anchored protein: an optical study, Biochemistry 32 (1993) 523–529.
[69] L.V. Shanshiashvili, N. Suknidze, G.G. Machaidze, D.G. Mikeladze, J.J. Ramsden, Adhesion and clustering of charge isomers of myelin basic protein at model myelin membranes, Arch. Biochem. Biophys. 419 (2003) 170–177.
[70] G. Vergeres, J.J. Ramsden, Regulation of the binding of myristoylated alanine-rich C kinase substrate (MARCKS) related protein to lipid bilayer membranes by calmodulin, Arch. Biochem. Biophys. 378 (2000) 45–50.
[71] A. Mashaghi, M. Swann, J. Popplewell, M. Textor, E. Reimhult, Optical anisotropy of supported lipid structures probed by waveguide spectroscopy and its application to study of supported lipid bilayer formation kinetics, Anal. Chem. 80 (2008) 3666–3676.
[72] D.J. Hirst, T.H. Lee, M.J. Swann, S. Unabia, Y. Park, K.S. Hahm, M.I. Aguilar, Effect of acyl chain structure and bilayer phase state on binding and penetration of a supported lipid bilayer by HPA3, Eur. Biophys. J. 40 (2011) 503–514.
[73] T.H. Lee, C. Heng, M.J. Swann, J.D. Gehman, F. Separovic, M.I. Aguilar, Real-time quantitative analysis of lipid disordering by aurein 1.2 during membrane adsorption, destabilisation and lysis, Biochim. Biophys. Acta 1798 (2010) 1977–1986.
[74] K. Hall, T.H. Lee, A.I. Mechler, M.J. Swann, M.I. Aguilar, Real-time measurement of membrane conformational states induced by antimicrobial peptides: balance between recovery and lysis, Sci. Rep. 4 (2014) 5479.
[75] S. Singh, P. Papareddy, M. Kalle, A. Schmidtchen, M. Malmsten, Importance of lipopolysaccharide aggregate disruption for the anti-endotoxic effects of heparin cofactor II peptides, Biochim. Biophys. Acta 1828 (2013) 2709–2719.
[76] M.M. Ouberai, J. Wang, M.J. Swann, C. Galvagnion, T. Guilliams, C.M. Dobson, M.E. Welland, alpha-Synuclein senses lipid packing defects and induces lateral expansion of lipids leading to membrane remodeling, J. Biol. Chem. 288 (2013) 20883–20895.
[77] R. Horvath, B. Kobzi, H. Keul, M. Moeller, E. Kiss, Molecular interaction of a new antibacterial polymer with a supported lipid bilayer measured by an in situ label-free optical technique, Int. J. Mol. Sci. 14 (2013) 9722–9736.
[78] T.H. Lee, K.N. Hall, M.J. Swann, J.F. Popplewell, S. Unabia, Y. Park, K.S. Hahm, M.I. Aguilar, The membrane insertion of helical antimicrobial peptides from the N-terminus of *Helicobacter pylori* ribosomal protein L1, Biochim. Biophys. Acta 1798 (2010) 544–557.
[79] R. Horvath, J.J. Ramsden, Quasi-isotropic analysis of anisotropic thin films on optical waveguides, Langmuir 23 (2007) 9330–9334.
[80] M.K. Baumann, M.J. Swann, M. Textor, E. Reimhult, Pleckstrin homology-phospholipase C-delta1 interaction with phosphatidylinositol 4,5-bisphosphate containing supported lipid bilayers monitored in situ with dual polarization interferometry, Anal. Chem. 83 (2011) 6267–6274.
[81] L.G. Yu, L. Guo, J.L. Ding, B. Ho, S.S. Feng, J. Popplewell, M. Swann, T. Wohland, Interaction of an artificial antimicrobial peptide with lipid membranes, Biochim. Biophys. Acta 2 (2009) 333–344.
[82] T.J. Zwang, W.R. Fletcher, T.J. Lane, M.S. Johal, Quantification of the layer of hydration of a supported lipid bilayer, Langmuir 26 (2010) 4598–4601.
[83] G.J. Hardy, R. Nayak, S. Zauscher, Model cell membranes: techniques to form complex biomimetic supported lipid bilayers via vesicle fusion, Curr. Opin. Colloid Interface Sci. 18 (2013) 448–458.
[84] C. Merz, W. Knoll, M. Textor, E. Reimhult, Formation of supported bacterial lipid membrane mimics, Biointerphases 3 (2008) FA41.
[85] B. Seantier, B. Kasemo, Influence of mono- and divalent ions on the formation of supported phospholipid bilayers via vesicle adsorption, Langmuir 25 (2009) 5767–5772.
[86] M. Montal, P. Mueller, Formation of bimolecular membranes from lipid monolayers and a study of their electrical properties, Proc Natl Acad Sci U S A 69 (1972) 3561–3566.
[87] J.F. Nagle, S. Tristram-Nagle, Structure of lipid bilayers, Biochim. Biophys. Acta 10 (2000) 159–195.
[88] S. Stanglmaier, S. Hertrich, K. Fritz, J.F. Moulin, M. Haese-Seiller, J.O. Radler, B. Nickel, Asymmetric distribution of anionic phospholipids in supported lipid bilayers, Langmuir 28 (2012) 10818–10821.
[89] H.P. Wacklin, Composition and asymmetry in supported membranes formed by vesicle fusion, Langmuir 27 (2011) 7698–7707.
[90] F.F. Rossetti, M. Textor, I. Reviakine, Asymmetric distribution of phosphatidyl serine in supported phospholipid bilayers, Langmuir 22 (2006) 3467–3473.
[91] Y. Jing, A. Kunze, S. Svedhem, Phase transition-controlled flip-flop in asymmetric lipid membranes, J. Phys. Chem. B 118 (2014) 2389–2395.
[92] N. Sanghera, M.J. Swann, G. Ronan, T.J. Pinheiro, Insight into early events in the aggregation of the prion protein on lipid membranes, Biochim. Biophys. Acta 1788 (2009) 2245–2251.
[93] V. Andreu-Fernandez, A. Genoves, T.H. Lee, M. Stellato, F. Lucantoni, M. Orzaez, I. Mingarro, M.I. Aguilar, E. Perez-Paya, Peptides derived from the transmembrane domain of Bcl-2 proteins as potential mitochondrial priming tools, ACS Chem. Biol. 9 (2014) 1799–1811.
[94] V. Balhara, R. Schmidt, S.U. Gorr, C. Dewolf, Membrane selectivity and biophysical studies of the antimicrobial peptide GL13K, Biochim. Biophys. Acta 1828 (2013) 2193–2203.

[95] J.C. Karst, R. Barker, U. Devi, M.J. Swann, M. Davi, S.J. Roser, D. Ladant, A. Chenal, Identification of a region that assists membrane insertion and translocation of the catalytic domain of *Bordetella pertussis* CyaA toxin, J. Biol. Chem. 287 (2012) 9200–9212.
[96] W.C. Wimley, Describing the mechanism of antimicrobial peptide action with the interfacial activity model, ACS Chem. Biol. 5 (2010) 905–917.
[97] S. Forbes, A.J. McBain, S. Felton-Smith, T.A. Jowitt, H.L. Birchenough, C.B. Dobson, Comparative surface antimicrobial properties of synthetic biocides and novel human apolipoprotein E derived antimicrobial peptides, Biomaterials 34 (2013) 5453–5464.
[98] S.B. Nielsen, D.E. Otzen, Impact of the antimicrobial peptide Novicidin on membrane structure and integrity, J. Colloid Interface Sci. 345 (2010) 248–256.
[99] T.H. Lee, C. Heng, F. Separovic, M.I. Aguilar, Comparison of reversible membrane destabilisation induced by antimicrobial peptides derived from Australian frogs, Biochim. Biophys. Acta 1838 (2014) 2205–2215.
[100] J. Zhai, T.H. Lee, D.H. Small, M.I. Aguilar, Characterization of early stage intermediates in the nucleation phase of Abeta aggregation, Biochemistry 51 (2012) 1070–1078.
[101] M.I. Aguilar, D.H. Small, Surface plasmon resonance for the analysis of beta-amyloid interactions and fibril formation in Alzheimer's disease research, Neurotox. Res. 7 (2005) 17–27.
[102] S. Devanathan, Z. Salamon, G. Lindblom, G. Grobner, G. Tollin, Effects of sphingomyelin, cholesterol and zinc ions on the binding, insertion and aggregation of the amyloid Abeta(1–40) peptide in solid-supported lipid bilayers, FEBS J. 273 (2006) 1389–1402.
[103] S. Henry, H. Vignaud, C. Bobo, M. Decossas, O. Lambert, E. Harte, I.D. Alves, C. Cullin, S. Lecomte, Interaction of Abeta(1–42) amyloids with lipids promotes "off-pathway" oligomerization and membrane damage, Biomacromolecules 16 (2015) 944–950.
[104] H.P. Ta, K. Berthelot, B. Coulary-Salin, S. Castano, B. Desbat, P. Bonnafous, O. Lambert, I. Alves, C. Cullin, S. Lecomte, A yeast toxic mutant of HET-s amyloid disrupts membrane integrity, Biochim. Biophys. Acta 1818 (2012) 2325–2334.
[105] L.P. Billen, C.L. Kokoski, J.F. Lovell, B. Leber, D.W. Andrews, Bcl-XL inhibits membrane permeabilization by competing with Bax, PLoS Biol. 6 (2008) e147.
[106] B. Leber, J. Lin, D.W. Andrews, Still embedded together binding to membranes regulates Bcl-2 protein interactions, Oncogene 29 (2010) 5221–5230.
[107] J.F. Lovell, L.P. Billen, S. Bindner, A. Shamas-Din, C. Fradin, B. Leber, D.W. Andrews, Membrane binding by tBid initiates an ordered series of events culminating in membrane permeabilization by Bax, Cell 135 (2008) 1074–1084.
[108] D.J. Hirst, T.H. Lee, M.J. Swann, M.I. Aguilar, Combined mass and structural kinetic analysis of multistate antimicrobial peptide–membrane interactions, Anal. Chem. 85 (2013) 9296–9304.
[109] D.J. Hirst, T.H. Lee, L.K. Pattenden, W.G. Thomas, M.I. Aguilar, Helix 8 of the angiotensin-II type 1a receptor interacts with phosphatidylinositol phosphates and modulates membrane insertion, Sci. Rep. (2015)http://dx.doi.org/10.1038/srep09972.
[110] M. Zasloff, Antimicrobial peptides of multicellular organisms, Nature 415 (2002) 389–395.
[111] S.A. Kotler, P. Walsh, J.R. Brender, A. Ramamoorthy, Differences between amyloid-beta aggregation in solution and on the membrane: insights into elucidation of the mechanistic details of Alzheimer's disease, Chem. Soc. Rev. 43 (2014) 6692–6700.